Article

Oxytree pruned biomass torrefaction - mathematical models of the influence of temperature and residence time on fuel properties improvement

Kacper Świechowski [1], Marek Liszewski [2], Przemysław Bąbelewski [3], Jacek A. Koziel [4], Andrzej Białowiec [1, 4]*

[1] Wrocław University of Environmental and Life Sciences, Faculty of Life Sciences and Technology, Institute of Agricultural Engineering, 37/41 Chełmońskiego Str., 51-630 Wrocław, Poland; kacper.swiechowski@upwr.edu.pl, andrzej.bialowiec@upwr.edu.pl

[2] Wrocław University of Environmental and Life Sciences, Faculty of Life Sciences and Technology, Institute of Agroecology and Plant Production, 24A pl. Grunwaldzki Str., 53-363 Wrocław, Poland, marek.liszewski@upwr.edu.pl

[3] Wrocław University of Environmental and Life Sciences, Faculty of Life Sciences and Technology, Department of Horticulture, 24A pl. Grunwaldzki Str., 53-363 Wrocław, Poland, przemyslaw.babelewski@upwr.edu.pl

[4] Department of Agricultural and Biosystems Engineering, Iowa State University, Ames, IA, USA: koziel@iastate.edu, andrzejb@iastate.edu

* Correspondence: andrzej.bialowiec@upwr.edu.pl; Tel.: +48-71-320-5973

Abstract: Biowaste generated in the process of Oxytree cultivation and logging represents a potential source of energy. Torrefaction (a.k.a. low-temperature pyrolysis) is one of the methods proposed for the valorization of woody biomass. Still, energy is required for the torrefaction process during which the raw biomass becomes biochar with fuel properties similar to lignite coal. In this work, models describing the influence of torrefaction temperature and residence time on the resulting fuel properties (mass and energy yields, energy densification ratio, organic matter and ash content, combustible parts, lower and higher heating values, CHONS content, H:C and O:C ratios) were proposed according to the Akaike criterion. The degree of the models' parameters matching the raw data expressed as the determination coefficient (R^2) ranged from 0.52 to 0.92. Each model parameter was statistically significant ($p<0.05$). Estimations of the value and quantity of the produced biochar from 1 Mg of biomass residues were made based on two models and a set of simple assumptions. The value of torrefied biochar (€123.4·Mg^{-1}) was estimated based on the price of commercially available coal fuel and its lower heating value (LHV) for biomass moisture content of 50%, torrefaction for 20 min at 200 °C. This research could be useful to inform techno-economic analyses and decision-making process pertaining to the valorization of pruned biomass residues.

Keywords: Biorenewable energy, pruning biomass, torrefaction, biochar, fuel properties, Oxytree, model

1. Introduction

The energy demand continues to increase, and researchers continue to develop alternative sources of energy. European Union directives aim to increase the share of renewable energy sources (RES) while lowering overall environmental impact. Renewable energy sources can have a positive impact on the environment and diversify energy supply. To date, ~10 % of energy) is derived from biomass on a global scale [1]. The EU aims to increase the biomass share in the RES up to 50 % [1]. By 2050, the share of RES in total energy consumption is expected to increase to 55-75 % [2]. Thus, the demand for RES, including wood-based biomass is expected to grow. At present, it is not feasible to completely replace fossil fuels with RES in a sustainable manner. There are concerns about the negative impact of increased energy demand from biomass on biodiversity and food security [3].

Preprints (www.preprints.org) | NOT PEER-REVIEWED | Posted: 13 June 2019 doi:10.20944/preprints201906.0126.v1

Peer-reviewed version available at Materials 2019, 12, ; doi:10.3390/ma12142228

However, introducing different biomass as feedstock could improve the biodiversity of energy crops. It is expected that the increase in the share of RES in the EU will lead to an increase in the demand for biomass from trees, which will lead to an increase in forested areas and short-rotation plantations [4].

Oxytree (*Paulownia Clon in Vitro 112*) has been considered as a relatively new plant suitable for short rotation because of its quick-growing characteristics and the ability to produce a significant amount of biomass. Oxytree biomass yield increases significantly in a relatively short time. For example, the dry mass of the tree can increase tenfold from 0.21 to 2.05 kg d.m. from the first to the second year since planting) [5]. Besides rapid growth, Oxytree is also more versatile than other energy crops. Oxytree's wood can be used as a non-construction building material for paper, furniture, instruments, and others [6]. This versatility of end users is of great importance in case of an unexpected drop in the demand for bioenergy; it also allows greater flexibility in meeting the needs of the energy and industrial sectors.

The Oxytree biomass yield depends on many factors, such as stocking density and climate. With estimated stocking of 3300 trees per hectare, the yield in the 5-y period can amount to 80 Mg·ha^{-1} d.m.; on average ~16 Mg·ha^{-1} d.m. per year [7]. Warm climates favored by paulownia can produce ~7.2-14.0 Mg·ha^{-1} d.m., with a planting density on a 3x2 m grid, 1666 ·ha^{-1} per hectare and 6000 m^3·ha^{-1} of irrigation in Andalusia [8].

Oxytree residues can be additionally utilized for energy purposes, similarly to the concept proposed by Dyjakon [10] for prunings from the apple orchard. The volume of plantation residues can be ~107 m^3 per hectare assuming that prunings consist of ~70% of the total tree volume and that ~250 m^3 of industrial wood can be obtained from 1 ha [9]. The application of torrefaction for the valorization of residual biomass fuel properties may increase the profitability and sustainability of energy production from the Oxytree biomass (Figure 1). To date, pruned biomass is typically left on the field, burned or composted on-site.

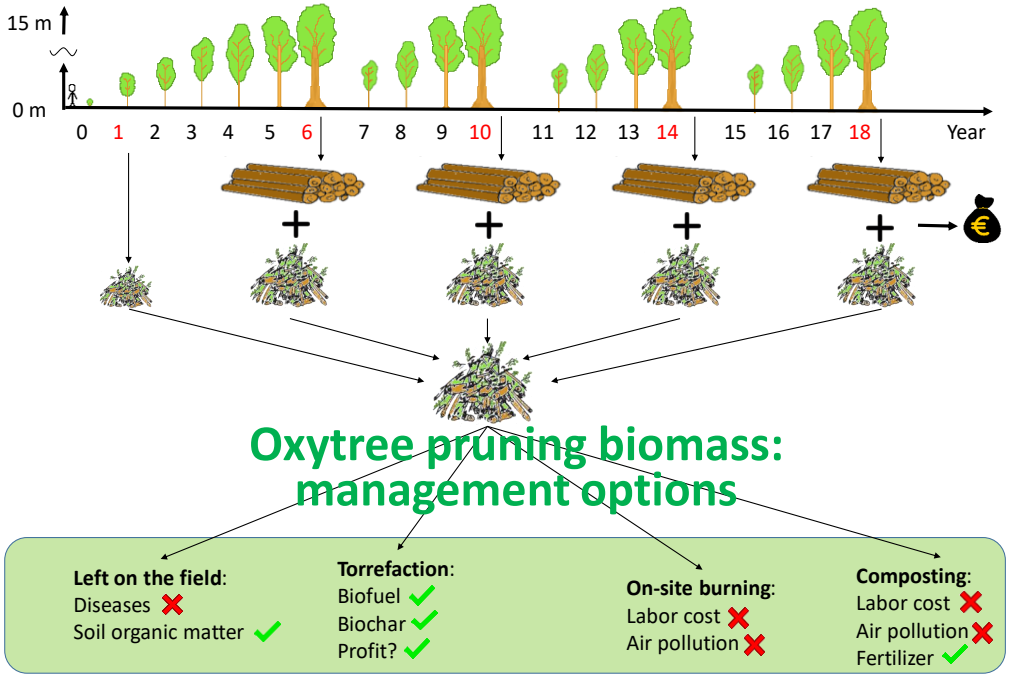

Figure 1. Graphic presentation of the current and proposed utilization of biomass residues on a plantation

Torrefaction, a.k.a. 'roasting' or 'mild pyrolysis,' is a thermochemical process with a limited amount of oxygen at ~near atmospheric pressure. The biomass is torrefied at a temperature of 200-300 °C at most up to 1 h. The purpose of the process is to obtain a material (called torrefied biomass or biochar) that has improved fuel properties than the substrate used for its production. During the biomass torrefaction, gases such as H_2, CO_2, CO, CH_4, C_xH_y, toluene, and benzene are produced in addition to steam, volatile organic compounds, and lipids. During the torrefaction, up to 30 % of the

Preprints (www.preprints.org) | NOT PEER-REVIEWED | Posted: 13 June 2019 doi:10.20944/preprints201906.0126.v1

Peer-reviewed version available at Materials 2019, 12, ; doi:10.3390/ma12142228

mass losses occur while maintaining 90% of the energy content of the substrate. These mass losses resulting from volatilization of condensable and non-condensable gases products [11,12].

Although the torrefaction process has been known for a long time, it has only recently become popular again because of the commencement of co-combustion of coal with biomass in some power plants. The torrefied biomass has a higher energy value, it contains less moisture, and it is easier to grind compared with raw biomass. By subjecting the biomass to torrefaction, it is possible to obtain biochar with fuel properties similar to lignite coal [13].

Cultivation of the Oxytree is critical to increasing the biomass yield (Figure 1). Pruning the tree at ~0.05 m above the ground in the middle of May (of the second growing season) is practiced to accelerate the growth and bring out a single straight trunk. During pruning, waste biomass is produced in the amount of 0.11-0.16 $Mg \cdot ha^{-1}$ d.m. (assuming 625 trees per hectare) [14]. Still, the amount of this biomass (30% by volume) may be too small for the energy-producing industry. However, after torrefaction, pruned biomass may be a source of additional income for growers in retail.

This research aimed at the determination of models for the influence of torrefaction temperature and process residence time on the torrefied biomass properties according to the Akaike criterion. Developed models may be used for the determination of the energetic potential of residues from pruning Oxytree and the techno-economic justification of using torrefaction for biomass valorization. In addition, the proposed models could be used to evaluate fuel properties from residues common in logging and horticulture industry because the pruned biomass is similar to common tree branches.

2. Materials and Methods

2.1. Models

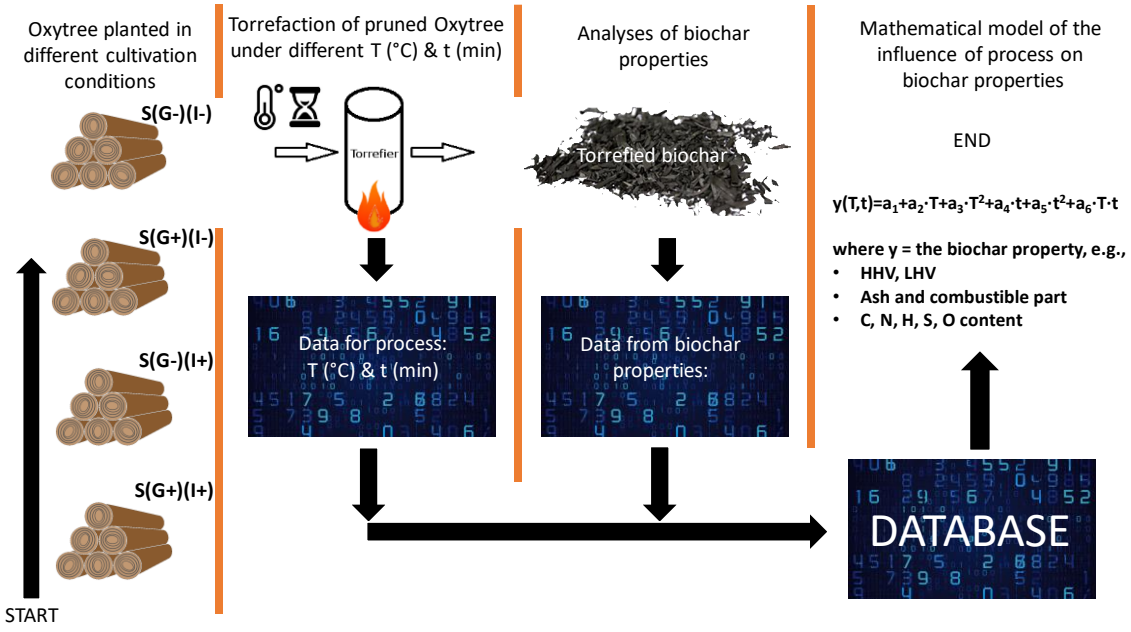

Figure 2. Diagram of experimental design and data evaluation.

The schematic diagram of the experiment and data treatment resulting in polynomial model parameters evaluation is shown in Figure 2. The experiment consisted of four elements: (1) Oxytree cultivation and pruning, (2) pruned biomass torrefaction, (3) determination of fuel properties of resulting biochars, and (4) estimation of parameters of a polynomial model describing the influence of torrefaction technological parameters (i.e., temperature, residence time) on fuel properties of biochars. The details of the experimental methodology of torrefaction process and obtained raw data were presented in the previous data article [14]. The data article contains the results of the pruned biomass process, the fuel properties of raw and torrefied biomass.

The pruned Oxytree biomass was originated from plantations cultivated under 8 different conditions of soil type, irrigation status, and geotextile. Oxytrees were grown on (S) sandy soil (classified as V soil belonging to brunic arenosols) and (C) clay soil (classified as Phaeozems), on which they were irrigated (N +) or not (N-), and had geotextile (G +) or not (G-) (Figure 2). The torrefaction was carried out at temperatures of 200-300 °C with an interval of 20 °C, at residence times 20, 40, and 60 min.

Polynomial models of influence of torrefaction temperature and biomass residence time in the torrefaction reactor on mass and energy efficiency of the torrefaction process, energy densification ratio, organic matter, combustible elements, ash, high heating value, low heating value, and elemental composition of torrefied biomass were built using the raw data [14]. The model parameters were estimated due to the non-linear regression analysis. Regression analysis used a 2-degree polynomial with a general form, with intercept (a_1) and 5 regression coefficients (a_{2-6}) (Equation 1).

$$f(T,t) = a_1 + a_2 \cdot T + a_3 \cdot T^2 + a_4 \cdot t + a_5 \cdot t^2 + a_6 \cdot T \cdot t \quad (1)$$

where:

f(T,t) - the biochar property obtained under T - temperature, and t – residence time conditions,

a_1 - intercept, -

a_{2-6} – regression coefficient, -

T - temperature, T = 200-300 °C,

t – residence time, t = 0-60 min.

The regression analysis was performed using the Statistica 12 software (StatSoft, Inc., TIBCO Software Inc. Palo Alto, CA, USA). For the determination of model parameters, the degree of matching to raw data, the determination coefficient (R^2) was calculated. The backward stepwise regression analysis was used for the reduction of insignificant parameters from the model in case of a lack of statistical significance ($p<0.05$). Then both models were compared with the Akaike analysis (AIC) to propose the simplest model with a similar matching to raw data. AIC was determined according to the least-squares method (Equation 2) [15]:

$$AIC = n \cdot ln(\sum_{i=1}^{n} e_i^2) + 2 \cdot K \quad (2)$$

where:

AIC – value of Akaike analysis, -,

n – the number of measurements, -,

e – the value of the rest of the model for particular measurements point, -,

K – number of regression coefficients including intercept (a_n) in model.

The assumption that a model with a lower AIC value describes the simpler model was used as a selection criterion of the better model.

3. Results

3.1. Models

The mass yield (*MY*) of the Oxytree torrefaction is shown in Figure 3. The MY decreased as the temperature and process time increased ($R^2 = 0.92$). The analysis of data reveals that the increase in temperature is more important to reduce *MY* than the residence time. The mass yield was ~50% for the torrefaction conditions (T, t) of 300 °C, 60 min. All regression coefficients of the model were statistically significant ($p<0.05$). The greatest positive impact on *MY* was associated with T ($\beta = 0.83$) and t^2 ($\beta = 0.56$). This positive impact was reduced by predictor T^2 ($\beta = -1.49$), t ($\beta = -0.19$), and T·t ($\beta = -0.74$), respectively.

Preprints (www.preprints.org) | NOT PEER-REVIEWED | Posted: 13 June 2019 doi:10.20944/preprints201906.0126.v1

Peer-reviewed version available at Materials 2019, 12, ; doi:10.3390/ma12142228

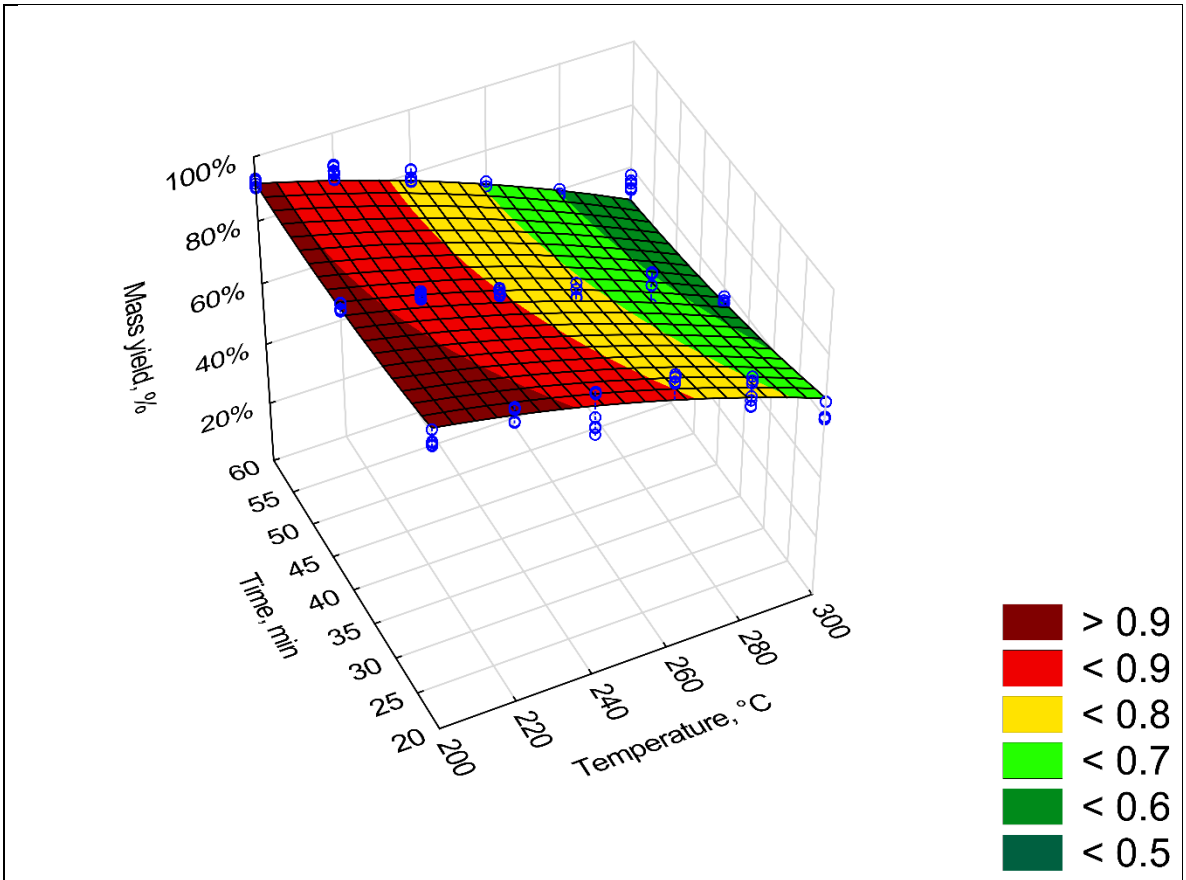

$MY = a_1+a_2 \cdot T+a_3 \cdot T^2+a_4 \cdot t+a_5 \cdot t^2+a_6 \cdot T \cdot t$, $R^2 = 0.92$

red font signifies statistical significance ($p < 0.05$)

Intercept/coefficient	Value of intercept/ coefficient	Standard error	p	Lower limit of confidence	Upper limit of confidence	Standardized β coefficient
a_1	0.891816	0.223378	0.00	0.450129	1.333503	-
a_2	0.003525	0.001746	0.00	0.000074	0.006977	0.83
a_3	-0.000013	0.000000	0.00	-0.000013	-0.000013	-1.49
a_4	-0.001684	0.002135	0.00	-0.005905	0.002538	-0.19
a_5	0.000062	0.000018	0.00	0.000025	0.000098	0.56
a_6	-0.000025	0.000000	0.00	-0.000025	-0.000025	-0.74

Figure 3. 3D model and statistical evaluation of mass yield (*MY*) of pruned biomass torrefaction.

The torrefaction process led to a reduction in the energy yield (*EY*) of the valorized material ($R^2 = 0.88$). As with MY, the temperature had a greater impact on lowering the energy yield value (Figure 4). The lowest value of *EY* (<70%) was achieved at 300 °C and 60 min. Each regression coefficient was statistically significant ($p<0.05$). The EY was affected by predictor T ($\beta = -2.35$) and T·t ($\beta = -1.16$). Because the predictor T^2 has the highest negative value, it is reasonable to assume that torrefaction temperature has the biggest impact on decreasing the *EY*.

Preprints (www.preprints.org) | NOT PEER-REVIEWED | Posted: 13 June 2019 doi:10.20944/preprints201906.0126.v1

Peer-reviewed version available at Materials 2019, 12, ; doi:10.3390/ma12142228

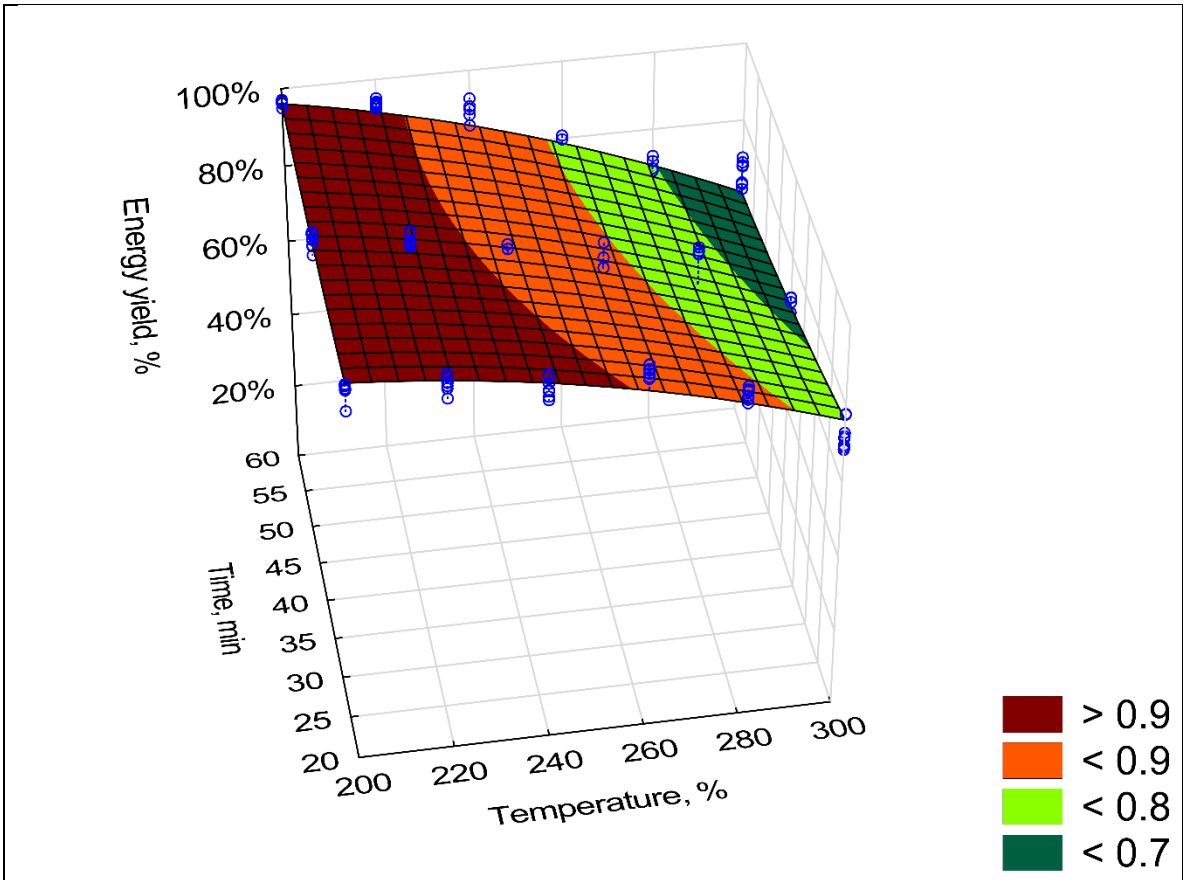

$EY = a_1+a_2 \cdot T+a_3 \cdot T^2+a_4 \cdot t+a_5 \cdot t^2+a_6 \cdot T \cdot t$, $R^2 = 0.88$

red font signifies statistical significance ($p < 0.05$)

Intercept/coefficient	Value of intercept/ coefficient	Standard error	p	Lower limit of confidence	Upper limit of confidence	Standardized β coefficient
a_1	0.429884	0.219439	0.00	-0.004012	0.863781	-
a_2	0.006285	0.001715	0.00	0.002894	0.009675	1.85
a_3	-0.000016	0.000000	0.00	-0.000016	-0.000016	-2.35
a_4	0.002472	0.002097	0.00	-0.001675	0.006619	0.35
a_5	0.000037	0.000018	0.00	0.000002	0.000073	0.42
a_6	-0.000031	0.000000	0.00	-0.000031	-0.000031	-1.16

Figure 4. 3D model and statistical evaluation of the energy yield (*EY*) of pruned biomass torrefaction.

The increase in energy densification ratio (*EDr*) in the biochar is one of the main advantages of the biomass torrefaction process. The *EDr* increased with the increase in the process T and its duration (Figure 5). The highest energy densification ratio value was ~1.21 for 300 °C and 60 min. The *EDr* model was characterized by a slightly lower R^2 (0.78) compared with *MY* and *EY*. Regression coefficients of the *EDr* model were statistically significant ($p<0.05$). The T^2 and t predictors had the greatest positive impact (β = 0.93 & 0.78, respectively). The T and t^2 predictors were negative (β = -0.18 and -0.7, respectively). Based on differences of β between predictors T^2 –T = 0.75, and t – t^2 = 0.08

Preprints (www.preprints.org) | NOT PEER-REVIEWED | Posted: 13 June 2019 doi:10.20944/preprints201906.0126.v1

Peer-reviewed version available at Materials 2019, 12, ; doi:10.3390/ma12142228

it can be concluded that temperature had a greater impact on *EDr* improvement than the process time.

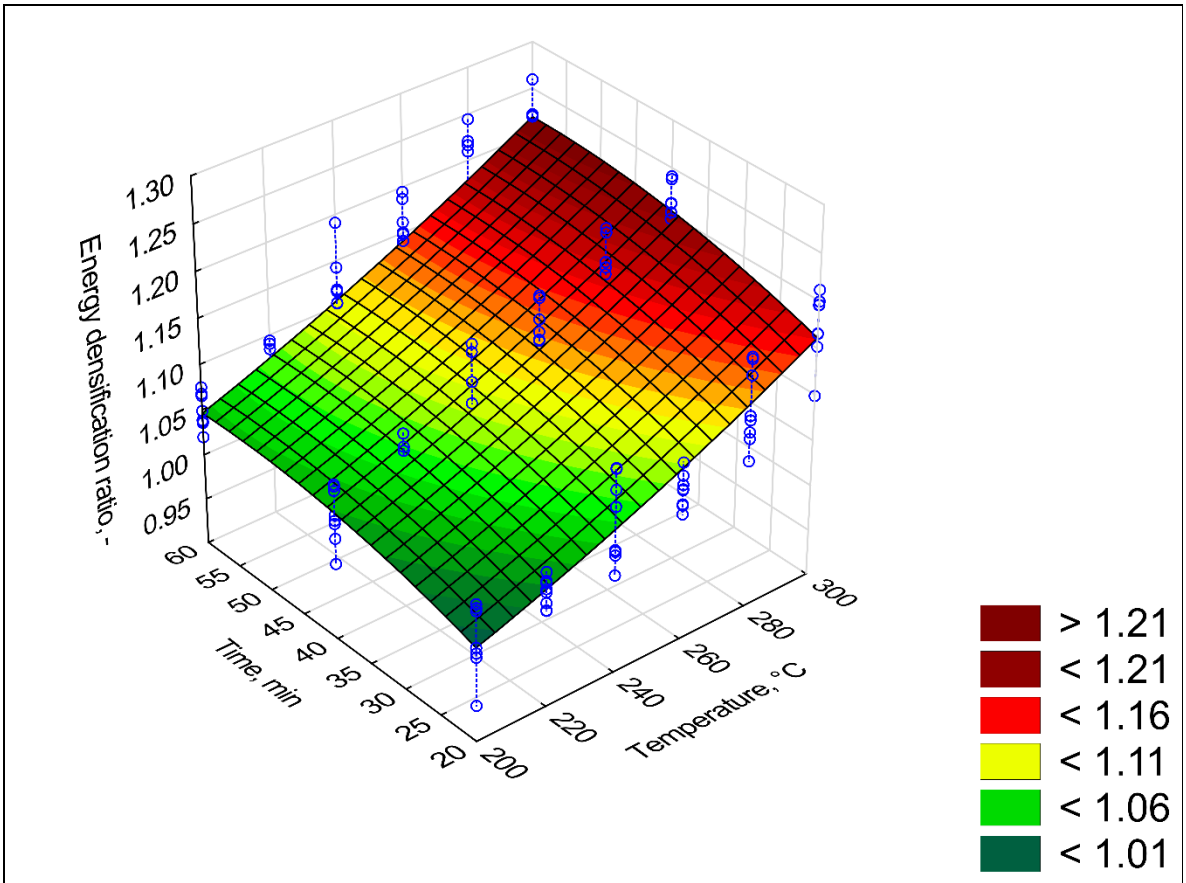

EDr = $a_1+a_2 \cdot T+a_3 \cdot T^2+a_4 \cdot t+a_5 \cdot t^2+a_6 \cdot T \cdot t$, $R^2 = 0.77$

red font signifies statistical significance ($p < 0.05$)

Intercept/coefficient	Value of intercept/ coefficient	Standard error	p	Lower limit of confidence	Upper limit of confidence	Standardized β coefficient
a_1	0.860189	0.182285	0.00	0.499756	1.220621	-
a_2	-0.000366	0.001424	0.00	-0.003183	0.002450	-0.18
a_3	0.000004	0.000000	0.00	0.000004	0.000004	0.93
a_4	0.003294	0.001742	0.00	-0.000151	0.006739	0.78
a_5	-0.000037	0.000015	0.00	-0.000066	-0.000007	-0.70
a_6	0.000004	0.000000	0.00	0.000004	0.000004	0.23

Figure 5. 3D model and statistical evaluation of energy densification ratio (*EDr*) of torrefied pruned biomass.

The highest organic matter content (*OM*) occurred in the biochar with the shortest process time and the lowest temperature of 200 °C (Figure 6). The *OM* content in the tested torrefied biomass ranged from 90% to 82%. Because of the large discrepancy in the results (blue vertical lines), the model has $R^2 = 0.61$. The regression coefficient of the model describing the organic matter are summarized in Figure 6. All regression coefficients of the equation were statistically significant (p

Preprints (www.preprints.org) | NOT PEER-REVIEWED | Posted: 13 June 2019 doi:10.20944/preprints201906.0126.v1

Peer-reviewed version available at Materials 2019, 12, ; doi:10.3390/ma12142228

<0.05). According to the standardized regression coefficient, predictors for T^2 and T·t had the greatest negative impact on *OM*. In this model, predictors T^2, t and t^2 contributed to the increase of *OM* value.

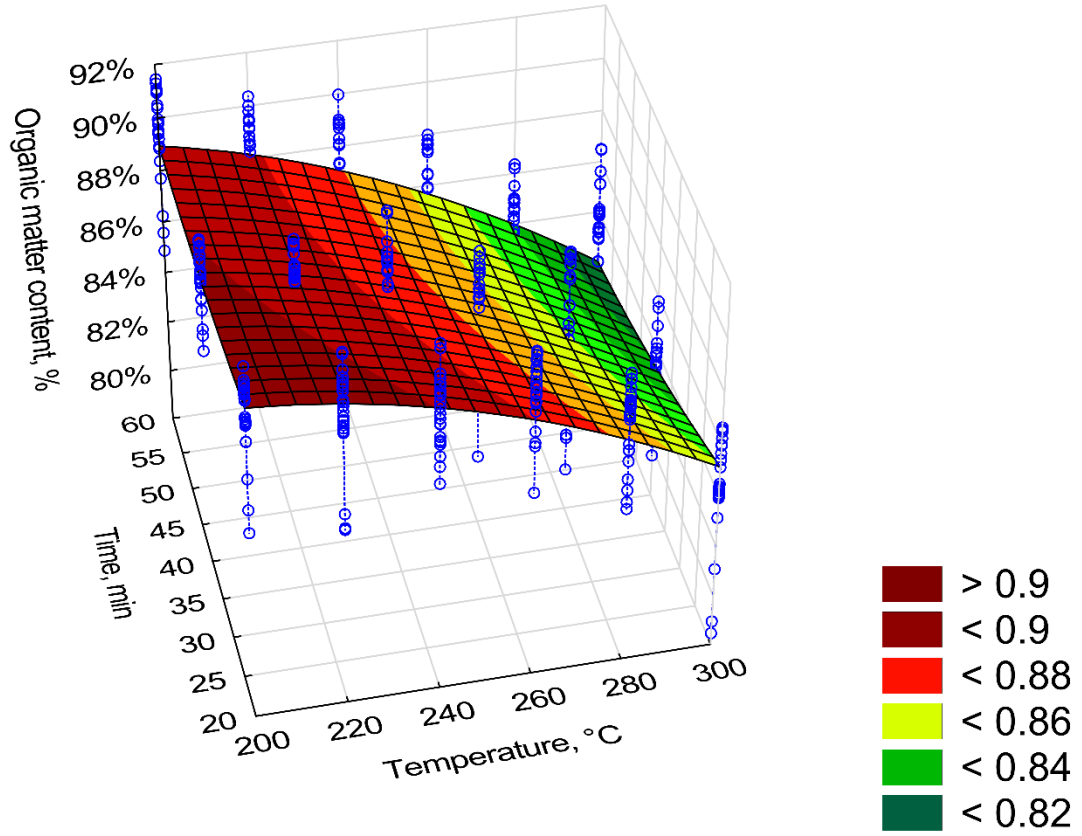

$OM = a_1+a_2 \cdot T+a_3 \cdot T^2+a_4 \cdot t+a_5 \cdot t^2+a_6 \cdot T \cdot t$, $R^2 = 0.59$

red font signifies statistical significance ($p < 0.05$)

Intercept/coefficient	Value of intercept/ coefficient	Standard error	p	Lower limit of confidence	Upper limit of confidence	Standardized β coefficient
a_1	0.764595	0.059289	0.00	0.648061	0.881130	-
a_2	0.001510	0.000463	0.00	0.000600	0.002421	1.76
a_3	-0.000004	0.000000	0.00	-0.000004	-0.000004	-2.21
a_4	0.000138	0.000567	0.00	-0.000976	0.001252	0.08
a_5	0.000008	0.000000	0.00	0.000008	0.000008	0.35
a_6	-0.000005	0.000000	0.00	-0.000005	-0.000005	-0.76

Figure 6. 3D model and statistical evaluation of organic matter (*OM*) content of torrefied pruned biomass.

Combustible part (*CP*) had a similar trend to that of *OM*. The *CP* content in the torrefied biomass decreased with t and with T increase. *CP* in the torrefied biomass decreased from 92% to 86% (Figure 7). The content of *CP* was inversely related to ash content (*AC*), i.e., as *CP* decreased, the *AC* (Figure 8) increased. The torrefied biomass was characterized by a high *AC* of up to 15%. The *CP* and *AC* models had poor fits ($R^2 = 0.53$) because there were significant deviations from mean values of up to 8% (straight blue lines on Figures 7 and 8). The regression coefficients of the *CP* and the *AC* models are presented in Figures 7 and 8, respectively. All regression coefficients of the equation were statistically significant ($p<0.05$) for both models. The standardized regression coefficients β in *CP*

Preprints (www.preprints.org) | NOT PEER-REVIEWED | Posted: 13 June 2019 doi:10.20944/preprints201906.0126.v1

Peer-reviewed version available at Materials 2019, 12, ; doi:10.3390/ma12142228

model had a similar trend as in *OM*; i.e., predictors T^2 and $T \cdot t$ had the greatest negative impact on *CP*. In the case of *AC* model, predictors T^2 and $T \cdot t$ had a positive impact ($\beta = 1.81$ and 0.6, respectively).

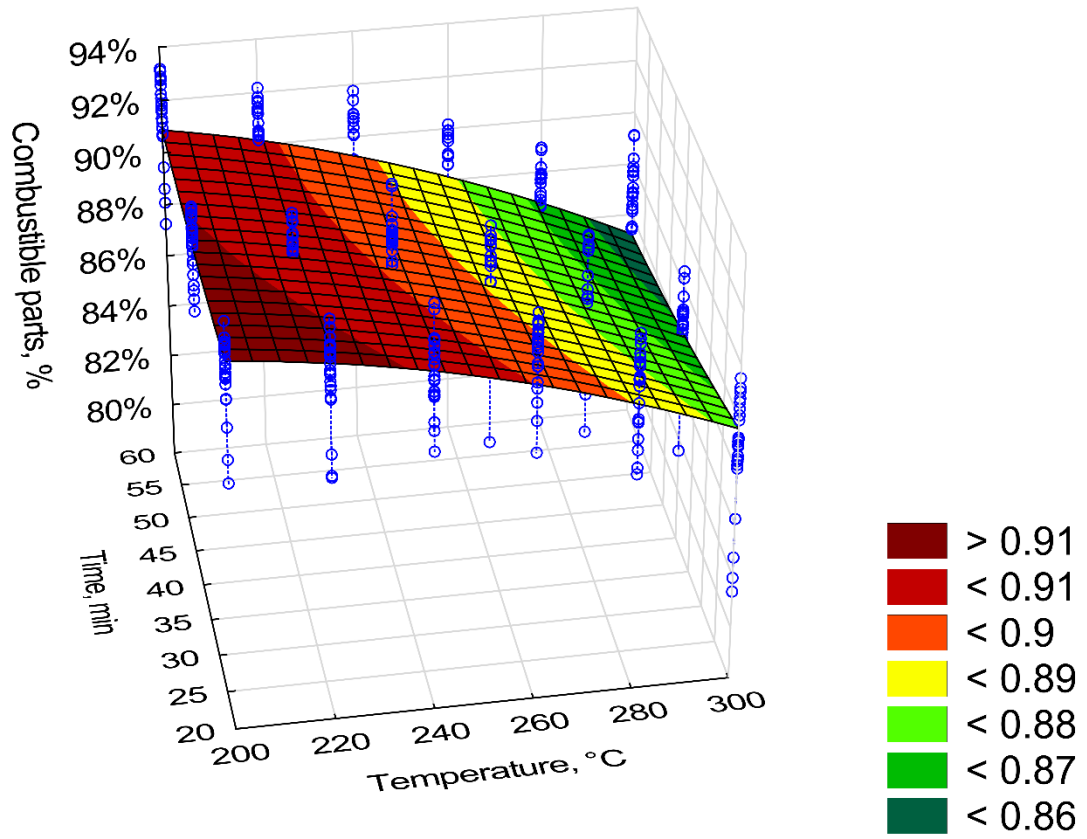

$CP = a_1 + a_2 \cdot T + a_3 \cdot T^2 + a_4 \cdot t + a_5 \cdot t^2 + a_6 \cdot T \cdot t$, $R^2 = 0.53$

red font signifies statistical significance ($p < 0.05$)

Intercept/coefficient	Value of intercept/ coefficient	Standard error	p	Lower limit of confidence	Upper limit of confidence	Standardized β coefficient
a_1	0.838668	0.054980	0.00	0.730603	0.946733	-
a_2	0.000997	0.000430	0.00	0.000152	0.001841	1.33
a_3	-0.000003	0.000000	0.00	-0.000003	-0.000003	-1.81
a_4	0.000029	0.000526	0.00	-0.001004	0.001062	0.02
a_5	0.000005	0.000000	0.00	0.000005	0.000005	0.28
a_6	-0.000004	0.000000	0.00	-0.000004	-0.000004	-0.60

Figure 7. 3D model and statistical evaluation of combustible part (*CP*) of pruned biomass.

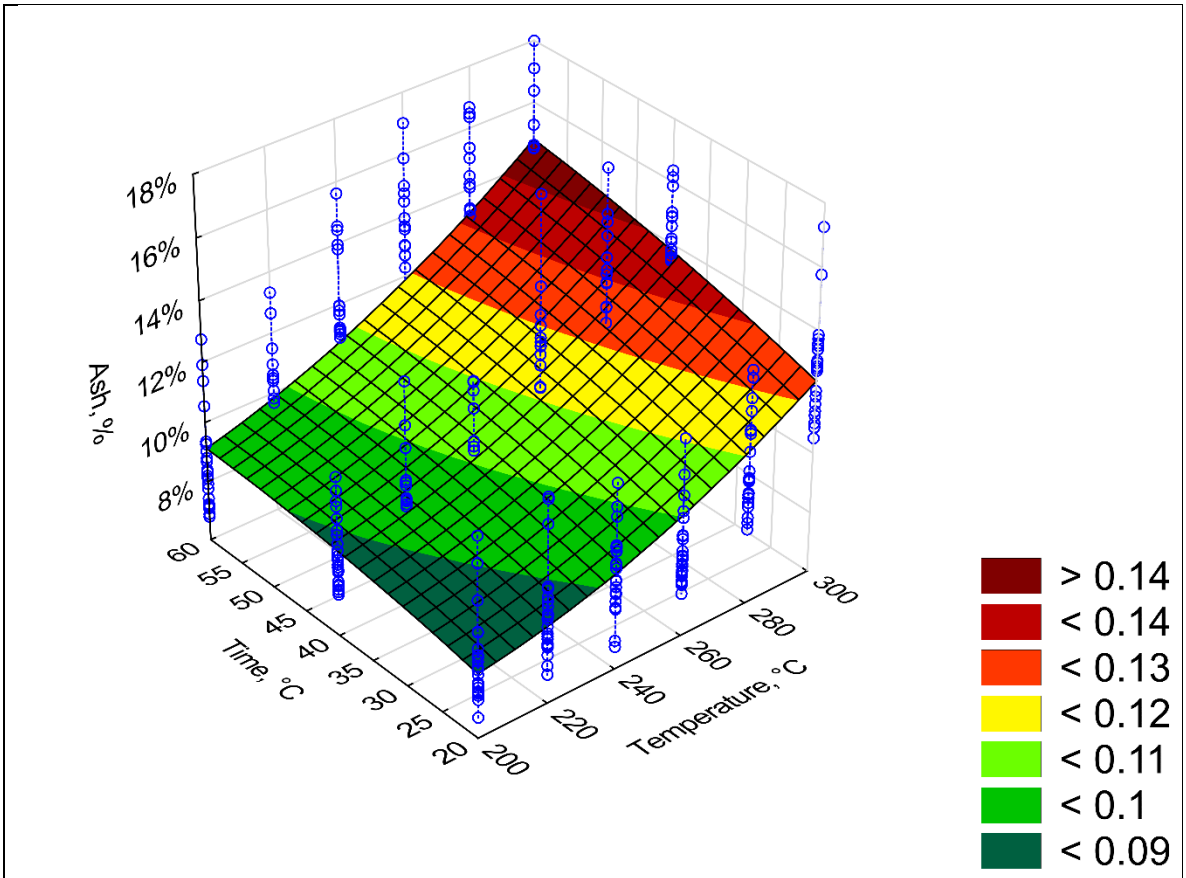

Ash (AC) = $a_1+a_2 \cdot T+a_3 \cdot T^2+a_4 \cdot t+a_5 \cdot t^2+a_6 \cdot T \cdot t$, $R^2 = 0.53$

red font signifies statistical significance ($p < 0.05$)

Intercept/coefficient	Value of intercept/ coefficient	Standard error	p	Lower limit of confidence	Upper limit of confidence	Standardized β coefficient
a_1	0.161333	0.054979	0.00	0.053268	0.269398	-
a_2	-0.000997	0.000430	0.00	-0.001841	-0.000152	-1.33
a_3	0.000003	0.000000	0.00	0.000003	0.000003	1.81
a_4	-0.000029	0.000525	0.00	-0.001062	0.001004	-0.02
a_5	-0.000005	0.000000	0.00	-0.000005	-0.000005	-0.28
a_6	0.000004	0.000000	0.00	0.000004	0.000004	0.60

Figure 8. 3D model and statistical evaluation of ash content (*AC*) of torrefied pruned biomass

The high heating value (*HHV*) increased with the process T and its duration increase (Figure 9). The highest *HHV* = 23 MJ·kg^{-1} value was recorded at 300 °C and 60 min [14], whereas the raw biomass had the *HHV* = 18.4 MJ·kg^{-1} [14]. The regression coefficients of *HHV* model are summarized in Figure 9. The a_2 and a_6 regression coefficients were not statistically significant ($p<0.05$) for $HHV=a_1+a_2 \cdot T+a_3 \cdot T^2+a_4 \cdot t+a_5 \cdot t^2+a_6 \cdot T \cdot t$ (model 1, Table A1). Consequently, they were removed from the analysis and the estimations were made again for the $HHV=a_1+a_2 \cdot T^2+a_4 \cdot t+a_5 \cdot t^2$ (model 2, Figure 9). There were practically no differences, between model (1) and (2) according to R^2 values. However, the Akaike analysis of both models revealed that the model (2) had the AIC lower by 2 compared with the model (1). Therefore, the model (2) with a lower value of AIC was chosen. According to standardized regression coefficient β, the t predictor had the greatest positive impact on *HHV* (β = 1). This positive effect of time was affected by predictor t^2 (β = -0.7). In this case, the predictor related to

Preprints (www.preprints.org) | NOT PEER-REVIEWED | Posted: 13 June 2019 doi:10.20944/preprints201906.0126.v1

Peer-reviewed version available at Materials 2019, 12, ; doi:10.3390/ma12142228

temperature T^2 ($\beta = 0.83$) had a greater impact on the *HHV* model, than predictors related to T. The same trends were observed for the *LHV* model (Figure 10).

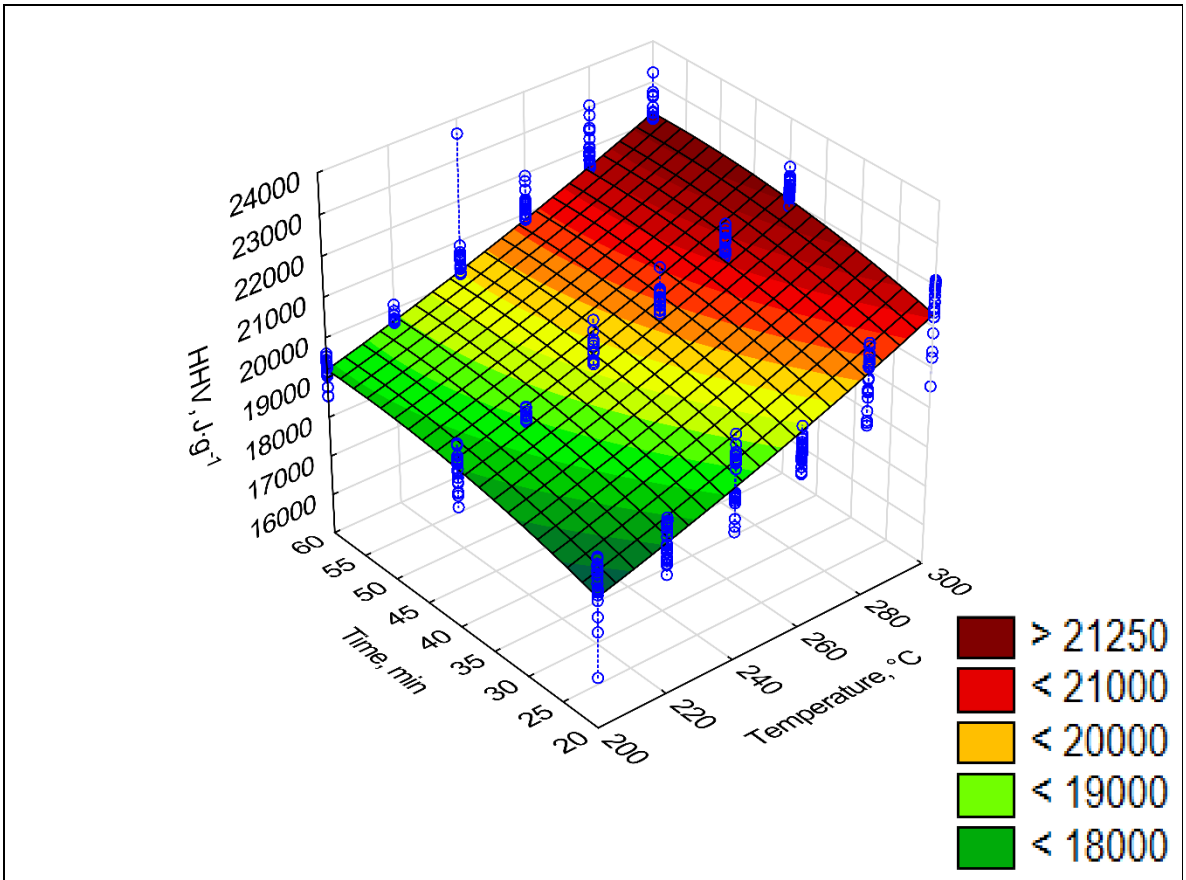

$HHV = a_1+a_2 \cdot T^2+a_3 \cdot t+a_4 \cdot t^2$, $R^2 = 0.79$, AIC = 8126

red font signifies statistical significance ($p < 0.05$)

Intercept/coefficient	Value of intercept/ coefficient	Standard error	p	Lower limit of confidence	Upper limit of confidence	Standardized β coefficient
a_1	14572.93	235.6392	0.000000	14109.78	15036.09	-
a_2	0.06	0.0016	0.000000	0.06	0.06	0.83
a_3	76.79	12.0003	0.000000	53.20	100.38	1.00
a_4	-0.67	0.1485	0.000009	-0.96	-0.38	-0.70

Figure 9. 3D model and statistical evaluation of *HHV* of torrefied pruned biomass (model 2)

The lower calorific value (*LHV*) increased with the increase of the process T and residence time (Figure 10). The *LHV* was found in torrefied biomass made at 200 °C and 220 °C and ranged from 16 to 20 $MJ \cdot kg^{-1}$, respectively [14]. The highest *LHV* resulted from torrefied biomass generated at 300 °C and 60 min. The regression coefficients of the *LVH* model are presented in Figure 10. Because in the model $LHV = a_1+a_2 \cdot T+a_3 \cdot T^2+a_4 \cdot t+a_5 \cdot t^2+a_6 \cdot T \cdot t$, the a_2 regression coefficient ($p < 0.05$) was not statistically significant (model 1, Table A2), the alternative model $LHV = a_1+a_2 \cdot T^2+a_3 \cdot t+a_4 \cdot t^2+a_5 \cdot T \cdot t$ was tested (model 2). Again, in this revised model, a_5 was not statistically significant (Table A3), so the model $LHV = a_1+a_2 \cdot T^2+a_3 \cdot t+a_4 \cdot t^2$ was tested (model 3). In model 3, all regression coefficients were statistically significant ($p < 0.05$). The R^2 values were almost the same in each model (~0.82). It can be assumed

Preprints (www.preprints.org) | NOT PEER-REVIEWED | Posted: 13 June 2019 doi:10.20944/preprints201906.0126.v1

Peer-reviewed version available at Materials 2019, 12, ; doi:10.3390/ma12142228

that the third model, compared to the first and second model, had a better fit because of AIC value. The first, second, and third model had an *AIC* of 8137, 8135, and 4904, respectively.

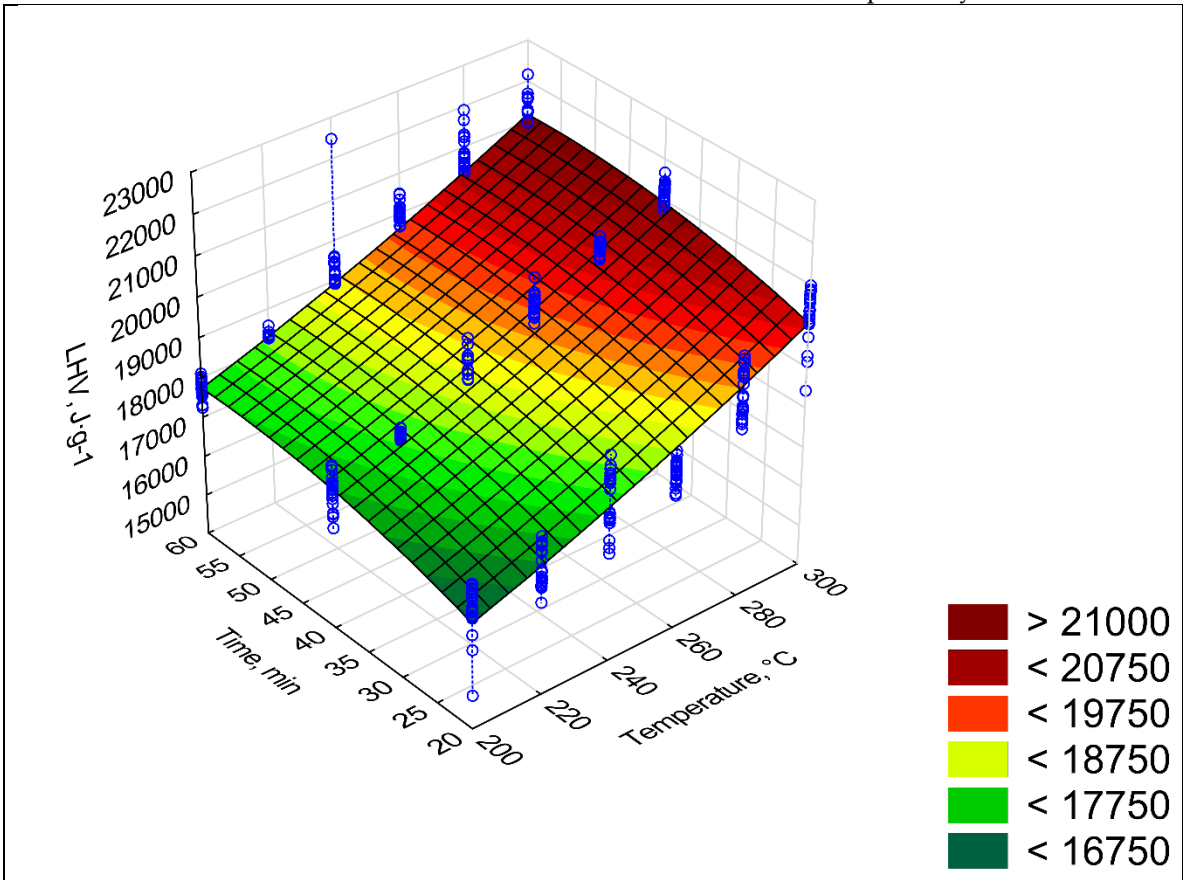

$LHV = a_1+a_2 \cdot T^2+a_3 \cdot t+a_4 \cdot t^2$, $R^2 = 0.82$, AIC = 4904

red font signifies statistical significance ($p < 0.05$)

Intercept/coefficient	Value of intercept/ coefficient	Standard error	p	Lower limit of confidence	Upper limit of confidence	Standardized β coefficient
a_1	12394.39	238.9256	0.000000	11924.77	12864.00	-
a_2	0.07	0.0017	0.000000	0.07	0.07	0.84
a_3	90.68	12.1676	0.000000	66.76	114.59	1.06
a_4	-0.79	0.1505	0.000000	-1.09	-0.50	-0.75

Figure 10. 3D model and statistical evaluation of *LHV* of torrefied pruned biomass (model 3)

Figures 11-15 present models of the C, H, N, S, O content in the torrefied biomass with R^2 ranging from 0.06 to 0.66. The highest R^2 was for the H model and the lowest for the S model. Relatively high $R^2 = 0.55$ was also noted for the O model. Other models had a coefficient of determination < 0.5. All regression coefficients were statistically significant ($p<0.05$) for each model (Figures 11-15). The C (Figure 11) and N (Figure 13) contents increased with the increase in T and t. The H (Figure 12) and O (Figure 15) contents had the opposite tends. The 3D model of S content (Figure 14) appears insensitive to T or t. Visible changes occurred above 250 °C and 40 min. The model, despite the statistically significant of all regression coefficients ($R^2 = 0.06$). A common finding for C, H, N, S, and O models was the value of standardized regression coefficients β. Predictors related to temperature

Preprints (www.preprints.org) | NOT PEER-REVIEWED | Posted: 13 June 2019 doi:10.20944/preprints201906.0126.v1

Peer-reviewed version available at Materials 2019, 12, ; doi:10.3390/ma12142228

(T, T^2) had a higher absolute value than those related to time (t, t^2). However, there was no link where predictors T and T^2 have a positive or negative value.

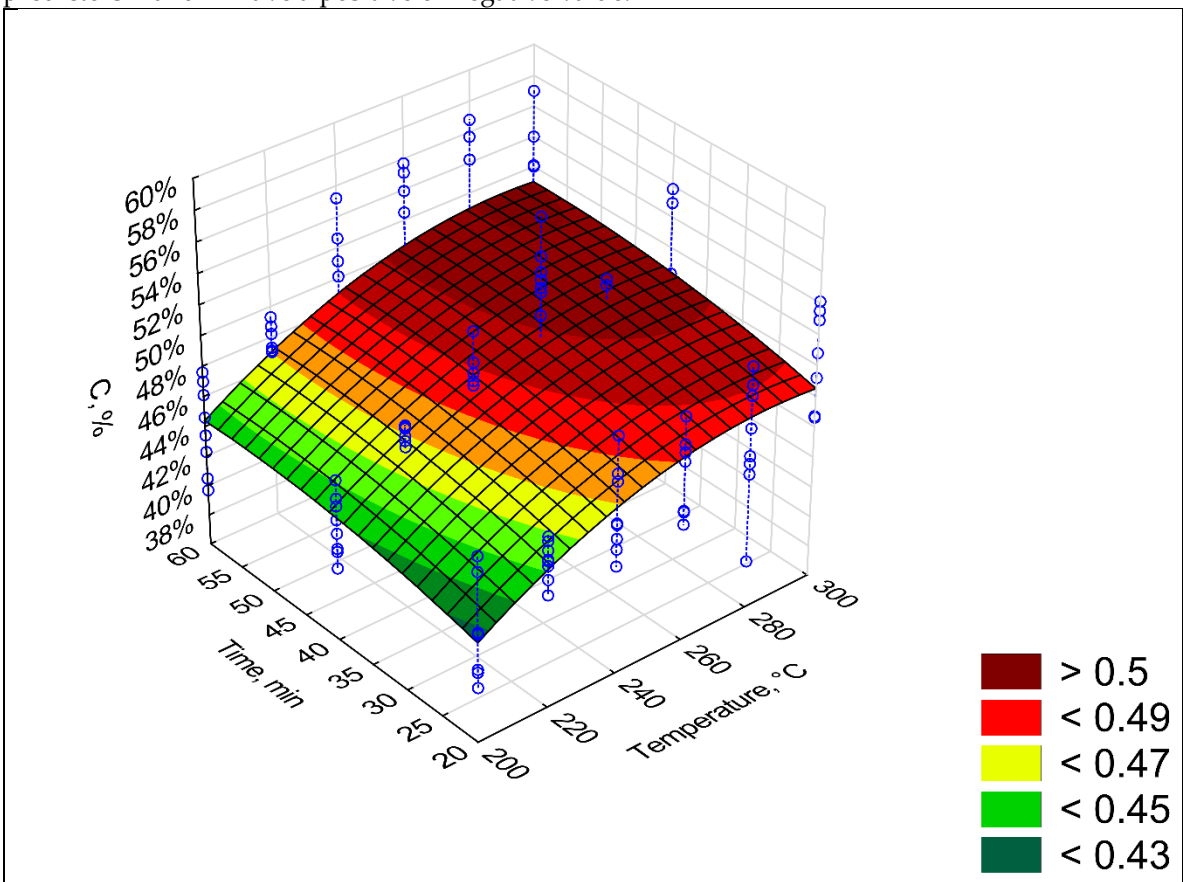

$C = a_1+a_2 \cdot T+a_3 \cdot T^2+a_4 \cdot t+a_5 \cdot t^2+a_6 \cdot T \cdot t$, $R^2 = 0.35$

red font signifies statistical significance ($p < 0.05$)

Intercept/coefficient	Value of intercept/ coefficient	Standard error	p	Lower limit of confidence	Upper limit of confidence	Standardized β coefficient
a_1	-0.212855	0.188451	0.00	-0.585480	0.159770	-
a_2	0.004700	0.001473	0.00	0.001788	0.007612	3.80
a_3	-0.000008	0.000000	0.00	-0.000008	-0.000008	-3.35
a_4	0.001477	0.001801	0.00	-0.002084	0.005039	0.57
a_5	-0.000017	0.000015	0.00	-0.000047	0.000014	-0.52
a_6	0.000002	0.000000	0.00	0.000002	0.000002	0.16

Figure 11. 3D model and statistical evaluation of C content of pruned biomass.

Preprints (www.preprints.org) | NOT PEER-REVIEWED | Posted: 13 June 2019 doi:10.20944/preprints201906.0126.v1

Peer-reviewed version available at Materials 2019, 12, ; doi:10.3390/ma12142228

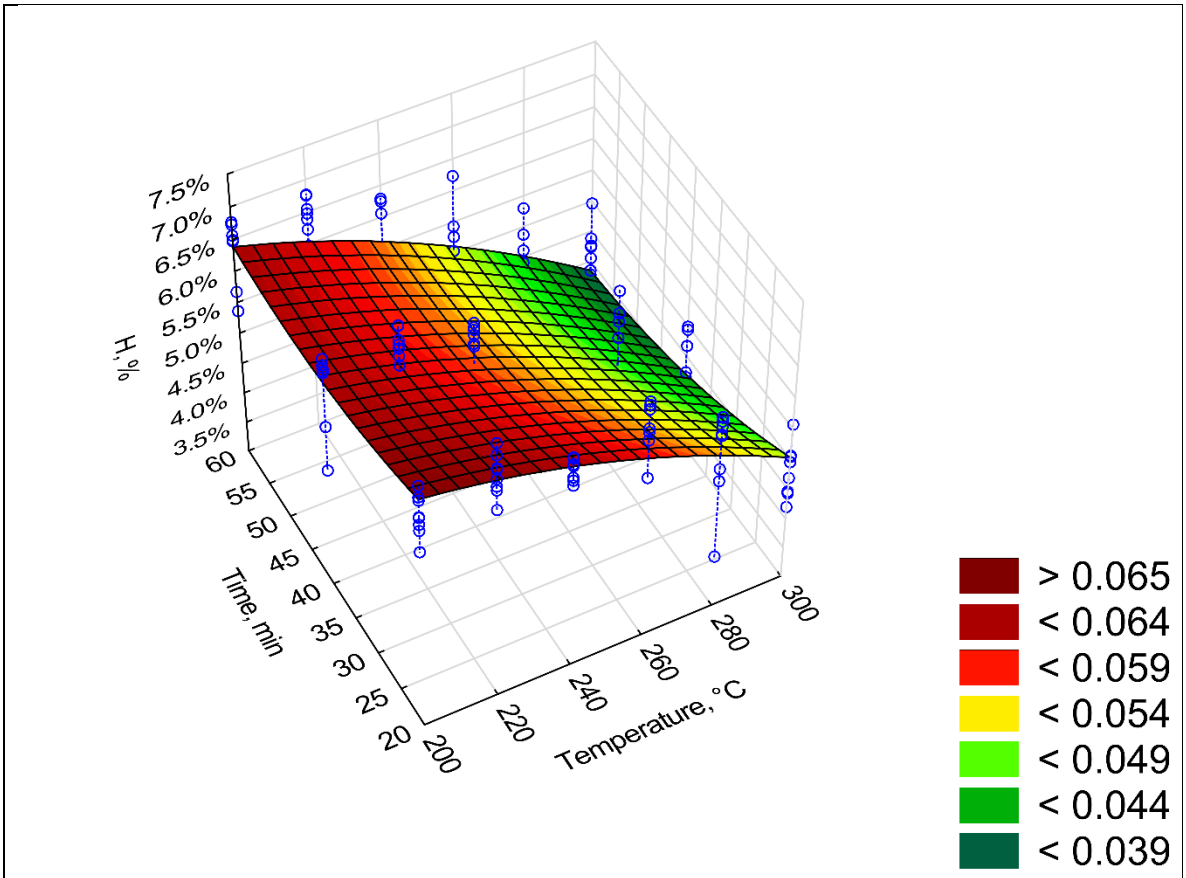

$H = a_1+a_2 \cdot T+a_3 \cdot T^2+a_4 \cdot t+a_5 \cdot t^2+a_6 \cdot T \cdot t$, $R^2 = 0.66$

red font signifies statistical significance ($p < 0.05$)

Intercept/coefficient	Value of intercept/ coefficient	Standard error	p	Lower limit of confidence	Upper limit of confidence	Standardized β coefficient
a_1	0.042265	0.032430	0.00	-0.021858	0.106388	-
a_2	0.000377	0.000253	0.00	-0.000124	0.000878	1.27
a_3	-0.000001	0.000000	0.00	-0.000001	-0.000001	-1.74
a_4	-0.000164	0.000310	0.00	-0.000777	0.000449	-0.27
a_5	0.000006	0.000000	0.00	0.000006	0.000006	0.75
a_6	-0.000002	0.000000	0.00	-0.000002	-0.000002	-0.85

Figure 12. 3D model and statistical evaluation of H content of pruned biomass.

Preprints (www.preprints.org) | NOT PEER-REVIEWED | Posted: 13 June 2019 doi:10.20944/preprints201906.0126.v1

Peer-reviewed version available at Materials 2019, 12, ; doi:10.3390/ma12142228

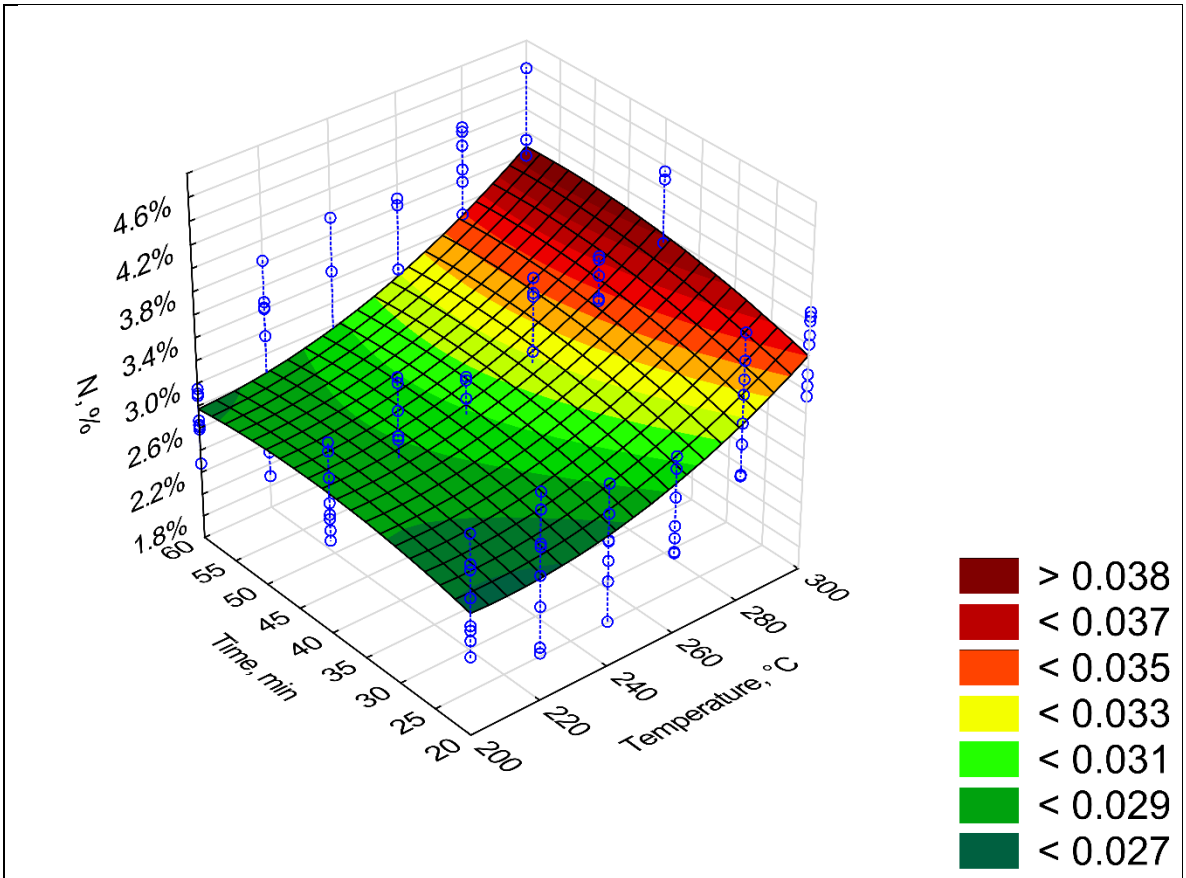

$N = a_1+a_2 \cdot T+a_3 \cdot T^2+a_4 \cdot t+a_5 \cdot t^2+a_6 \cdot T \cdot t$, $R^2 = 0.41$

red font signifies statistical significance ($p < 0.05$)

Intercept/coefficient	Value of intercept/ coefficient	Standard error	p	Lower limit of confidence	Upper limit of confidence	Standardized β coefficient
a_1	0.068473	0.023985	0.00	0.021047	0.115899	-
a_2	-0.000429	0.000187	0.00	-0.000800	-0.000059	-2.59
a_3	0.000001	0.000000	0.00	0.000001	0.000001	3.01
a_4	0.000134	0.000229	0.00	-0.000319	0.000588	0.39
a_5	-0.000003	0.000000	0.00	-0.000003	-0.000003	-0.71
a_6	0.000001	0.000000	0.00	0.000001	0.000001	0.51

Figure 13. 3D model and statistical evaluation of N content of pruned biomass.

Preprints (www.preprints.org) | NOT PEER-REVIEWED | Posted: 13 June 2019 doi:10.20944/preprints201906.0126.v1

Peer-reviewed version available at Materials 2019, 12, ; doi:10.3390/ma12142228

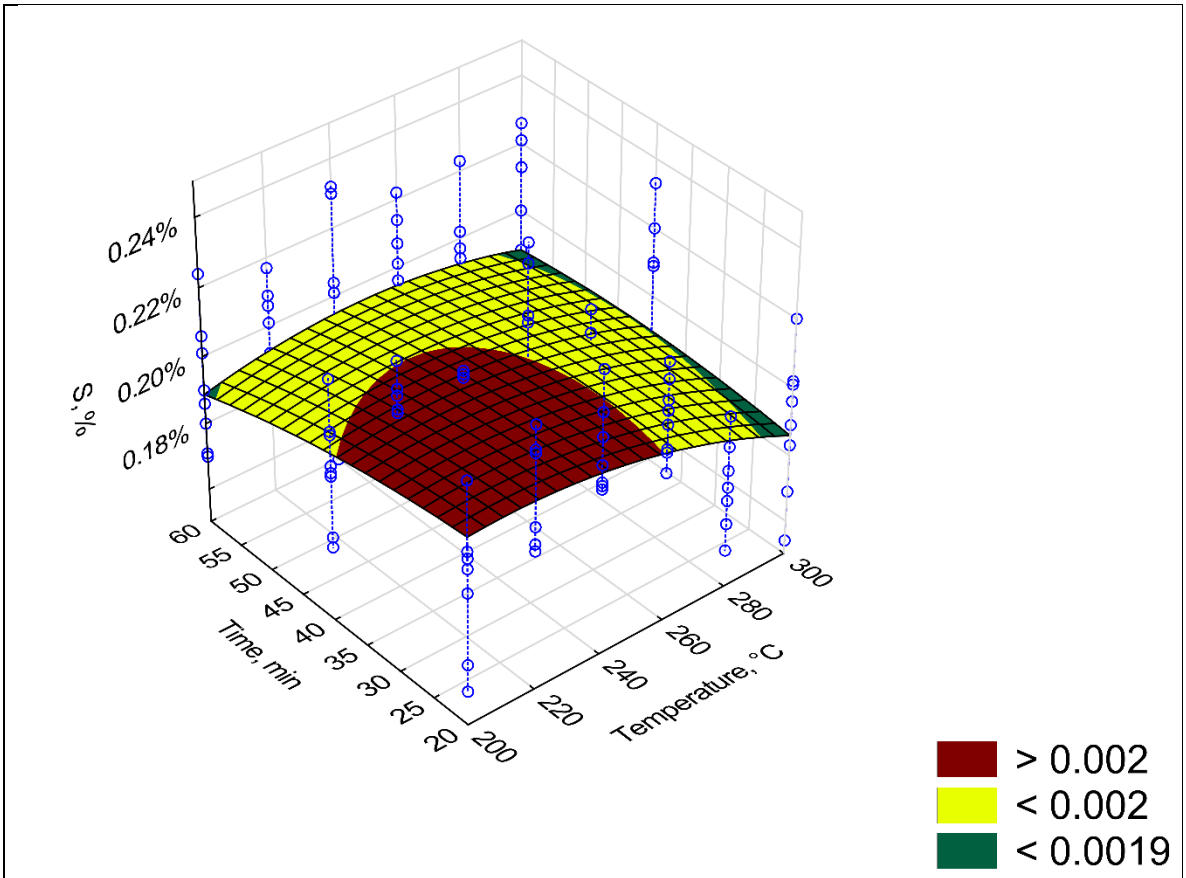

$S = a_1+a_2 \cdot T+a_3 \cdot T^2+a_4 \cdot t+a_5 \cdot t^2+a_6 \cdot T \cdot t$, $R^2 = 0.06$

red font signifies statistical significance ($p < 0.05$)

Intercept/coefficient	Value of intercept/ coefficient	Standard error	p	Lower limit of confidence	Upper limit of confidence	Standardized β coefficient
a_1	0.001055	0.001325	0.00	-0.001566	0.003676	-
a_2	0.000010	0.000010	0.00	-0.000010	0.000031	1.41
a_3	0.000000	0.000000	0.00	0.000000	0.000000	-1.81
a_4	-0.000008	0.000013	0.00	-0.000033	0.000017	-0.52
a_5	0.000000	0.000000	0.00	0.000000	0.000000	-0.36
a_6	0.000000	0.000000	0.00	0.000000	0.000000	0.81

Figure 14. 3D model and statistical evaluation of S content of pruned biomass.

Preprints (www.preprints.org) | NOT PEER-REVIEWED | Posted: 13 June 2019 doi:10.20944/preprints201906.0126.v1

Peer-reviewed version available at Materials 2019, 12, ; doi:10.3390/ma12142228

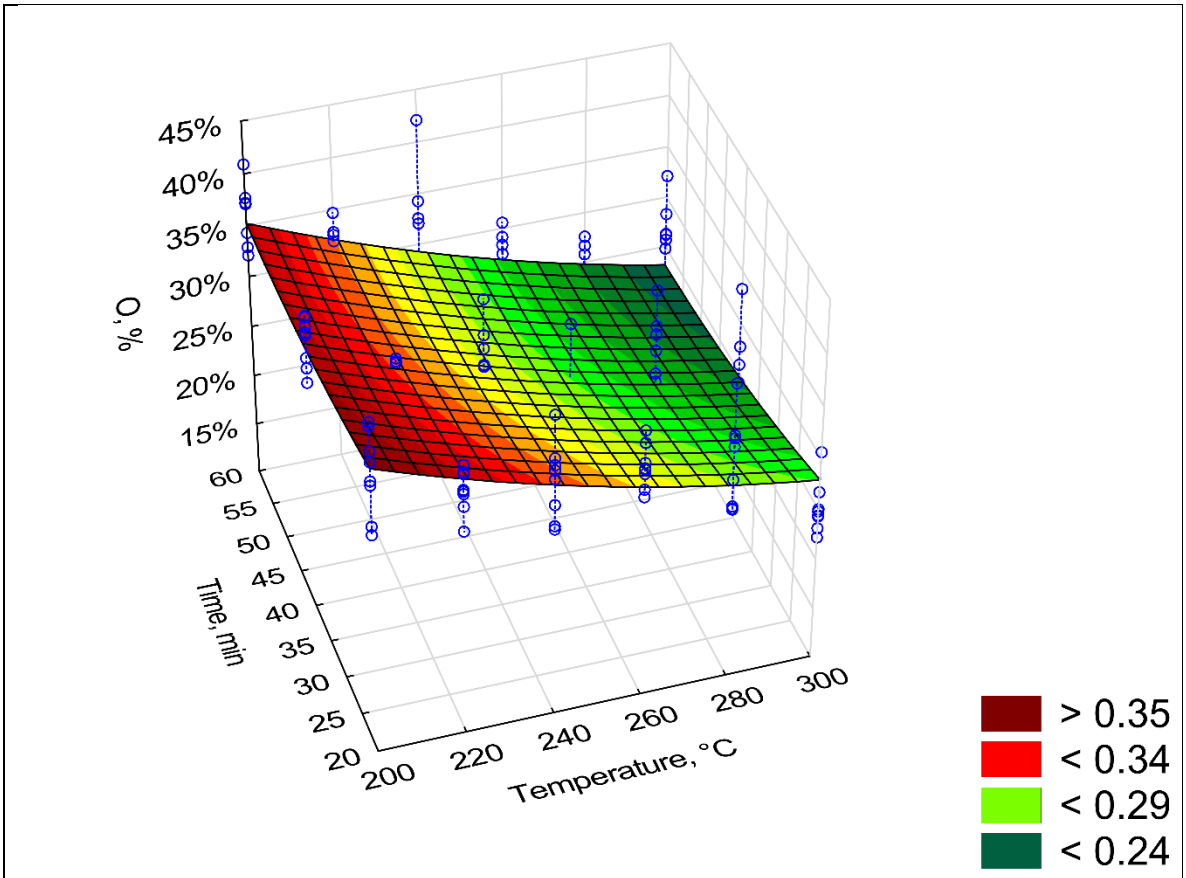

$O = a_1+a_2 \cdot T+a_3 \cdot T^2+a_4 \cdot t+a_5 \cdot t^2+a_6 \cdot T \cdot t$, $R^2 = 0.55$

red font signifies statistical significance ($p < 0.05$)

Intercept/coefficient	Value of intercept/ coefficient	Standard error	p	Lower limit of confidence	Upper limit of confidence	Standardized β coefficient
a_1	0.873544	0.207078	0.00	0.464088	1.283001	-
a_2	-0.003199	0.001618	0.00	-0.006398	0.000001	-1.96
a_3	0.000005	0.000000	0.00	0.000005	0.000005	1.42
a_4	-0.001367	0.001979	0.00	-0.005280	0.002547	-0.40
a_5	0.000022	0.000017	0.00	-0.000011	0.000055	0.52
a_6	-0.000005	0.000000	0.00	-0.000005	-0.000005	-0.41

Figure 15. 3D model and statistical evaluation of O content of pruned biomass.

Figures 16-17 depict changes in the value of *H:C* and *O:C* ratios depending on the T and t time. Model of *H:C* ratio (Figure 16) was characterized by high R^2 (0.82), while *O:C* ratio model had R^2 of 0.48. The first model of *H:C* ratio (model 1) had 3 statistically insignificant regression coefficients ($p < 0.05$), $R^2 = 0.82$, and *AIC* = 164 (Table A4). Non-significant regression coefficients have been removed and the second model has been proposed (model 2, Figure 16). The second model has the same $R^2 = 0.82$, yet with a higher *AIC* = 200 (Figure 15). Elevated the temperature and process time led to a reduction of *H:C* ratio from about 1.5 to 0.9 for 300 °C at 20 min and 300 °C at 60 min, respectively. The same change in conditions caused a change in *O:C* ratio from ~0.47 to 0.37. In the *H:C* ratio model predictor t^2 has a positive impact ($\beta = 1.68$) on the value of *H:C* ratio. However, the predictor T·t had a greater

negative impact (β = -2.15). With the *O:C* ratio model, the most significant impact had a predictor related to the T for which β = -3.03.

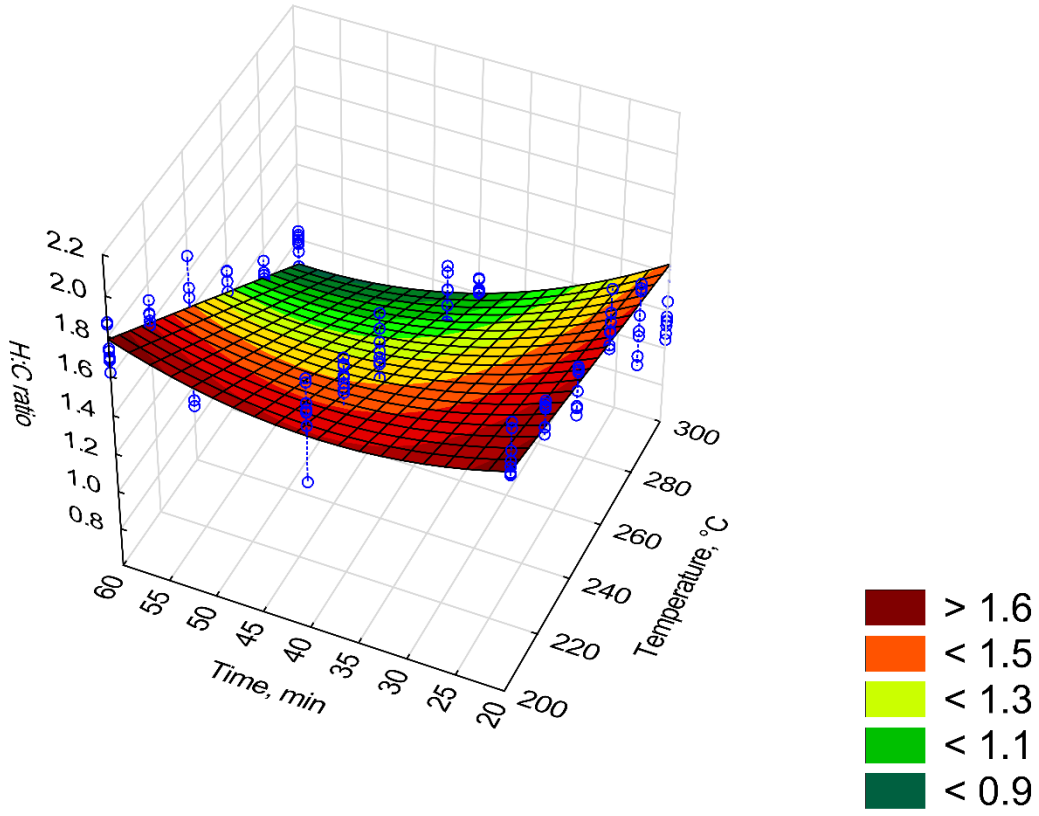

$H:C = a_1+a_2 \cdot t^2+a_3 \cdot T \cdot t$, $R^2 = 0.82$, AIC = 200

red font signifies statistical significance ($p < 0.05$)

Intercept/coefficient	Value of intercept/ coefficient	Standard error	p	Lower limit of confidence	Upper limit of confidence	Standardized β coefficient
a_1	2.207455	0.044156	0.00	2.120162	2.294748	-
a_2	0.000394	0.000029	0.00	0.000338	0.000451	1.68
a_3	-0.000153	0.000000	0.00	-0.000153	-0.000153	-2.15

Figure 16. 3D model and statistical evaluation of *H:C* ratio of pruned biomass (model 2)

Preprints (www.preprints.org) | NOT PEER-REVIEWED | Posted: 13 June 2019 doi:10.20944/preprints201906.0126.v1

Peer-reviewed version available at Materials 2019, 12, ; doi:10.3390/ma12142228

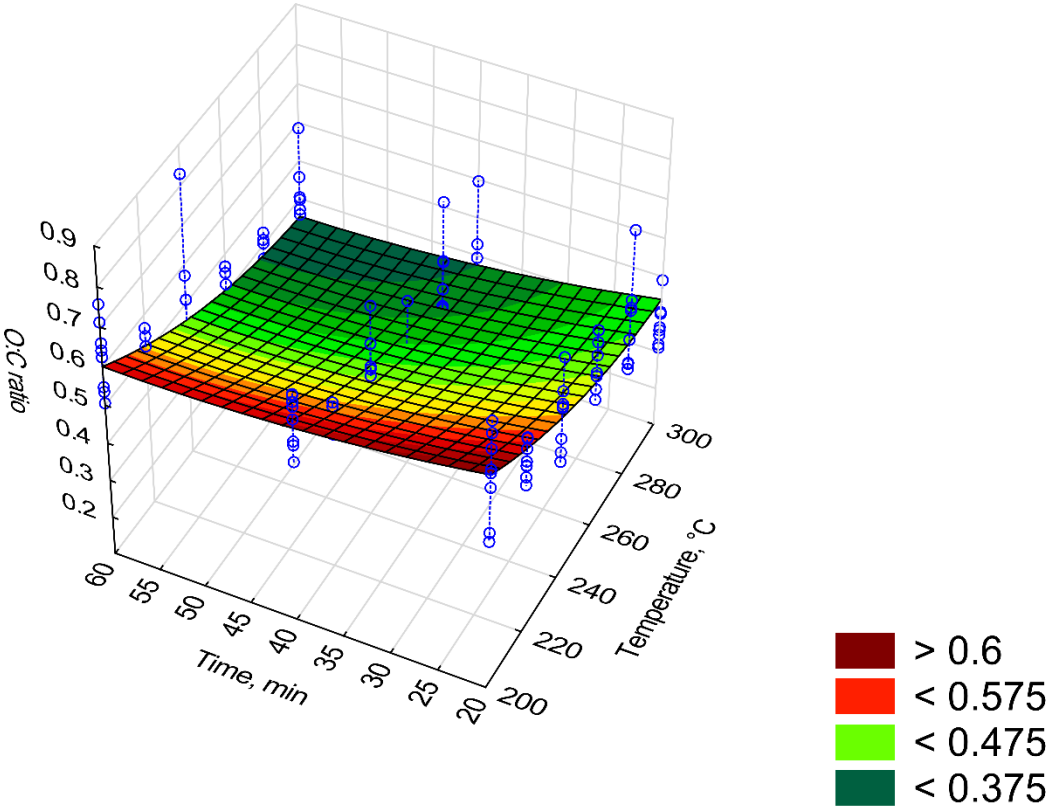

$O{:}C = a_1+a_2 \cdot T+a_3 \cdot T^2+a_4 \cdot t+a_5 \cdot t^2+a_6 \cdot T \cdot t$, $R^2 = 0.48$

red font signifies statistical significance ($p < 0.05$)

Intercept/coefficient	Value of intercept/ coefficient	Standard error	p	Lower limit of confidence	Upper limit of confidence	Standardized β coefficient
a_1	0.022935	0.005095	0.00	0.012860	0.033010	-
a_2	-0.000114	0.000040	0.00	-0.000192	-0.000035	-3.03
a_3	0.000000	0.000000	0.00	0.000000	0.000000	2.47
a_4	-0.000047	0.000049	0.00	-0.000143	0.000050	-0.59
a_5	0.000001	0.000000	0.00	0.000001	0.000001	0.55
a_6	0.000000	0.000000	0.00	0.000000	0.000000	-0.21

Figure 17. 3D model and statistical evaluation of O:C ratio of pruned biomass

4. Discussion

4.1. Models

The mass and energy yield (*MY* and *EY*) of the torrefaction process decrease with increasing T and t. The *MY* and *EY* values for Oxytree are in the range of other biochars derived from wood biomass. At temperatures of 275 ° C and 300 °C (60 min), the *MY* value for spruce was ~70 % and ~50 % [16], i.e., corresponding to those reported in Figure 1. At temperatures of 275 °C and 300 °C (60 min), the *MY* value for spruce was ~70 % and ~50 % [16], i.e., corresponding to those reported in Figure 1. For willow torrefeid in 15 min at a 250 °C the *MY* was 70 % [17]. It is much less than for torrefied pruned biomass of oxytree for which *MY* at 250 °C, 20 min was 90 % (Figure 1). The *MY* and *EY* in the case of torrefied willow at a process temperature of 230-290 °C was 95-72 %, and *EY* was 97-79 % [18]. In the case of Oxytree, these values ranged from 90-50 % and 90-70%, respectively (Figures 3 and 4). Energy efficiency for spruce torrefaction at 225-300 °C was between 93-68 %, and the *EDr* at 300 °C was 1.2 [19], i.e., the same as for the pruned torrefied Oxytree biomass (Figure 5).

The models for *MY*, *EY*, and *EDr* were characterized by a high determination coefficient R^2 of 0.78-0.92, which means that the proposed models can be considered suitable for describing the torrefaction of pruned biomass from a cultivation treatment.

The content of *OM* in the torrefied Oxytree ranged from 90 to 80%. The model describing the value of *OM* has a relatively low R^2 (0.63). The decrease in the *OM* results from the decomposition of organic compounds under the influence of T and their degassing (torgas). The lower fit of the model to the data was likely due to the high variability of empirical data around the average (illustrated with the blue vertical lines). Nevertheless, it shows accurately the tends of the *OM* loss along with the increase of T and t.

Similar low coefficients of determination were obtained for the *CP* and *AC* (R^2=0.53). This was similar, as in the case of *OM*, because of the large variation in measurement data. *CP* is associated with the ash content. As the *CP* decreases, the *AC* increases. Torrefaction causes a decrease in *CP* and an increase in *AC*. It is associated with the degassing of combustibles that are released during the torrefaction process. The *AC* in the torrefied pruned Oxytree biomass ranged from 7 % to 14 % [14]. This is a much higher value than that found in torrefied wood from torrefied pine 0.15-0.21 % [20] and birch 0.23-0.38 % [21]. The AC values obtained for Oxytree was closer to the corn stover 10-12 % [22]. The model of $HHV=a_1+a_2 \cdot T^2+a_4 \cdot t+a_5 \cdot t^2$ form was better than $HHV=a_1+a_2 \cdot T+a_3 \cdot T^2+a_4 \cdot t+a_5 \cdot t^2+a_6 \cdot T \cdot t$ because has a lower number of parameters, so it is easier to use. In addition, the model has a lower AIC value. The differences were insignificant, but the shorter model has an *AIC* of 8126 compared to 8128, whereas the R^2 is almost the same for both.

The *LHV* of the torrefied pruned Oxytree biomass at 270 °C and 30 min was over 21.5 $MJ \cdot kg^{-1}$ (Figure 9) and is comparable with the calorific value of willow torrefied in the same conditions [23]. The calorific value of the torrefaction from the pruned Oxytree biomass generated at 265 °C and 60 min was above 20 $MJ \cdot kg^{-1}$ (Figure 10). This value is ~1-3 $MJ \cdot kg^{-1}$ lower than in the case of torrefied eucalyptus, poplar, and pine at 265 °C and 105 min [24].

Models describing the change in the content of elements suggest that increasing the torrefaction T leads to an increase in the C content and a decrease in the content of O and H. An interesting tendency can be observed in the N model, i.e., the amount of N increased with increasing T and t. This finding is opposite to the typical N content [25] [26]. The S model is not comparable because its R^2 = 0.06. During the torrefaction process, the decrease in O and H content is mainly due to the weakness of bonded structures such as -OH [27]. Similarly, a drop in N content should be observed due to losses of weakly bonded structures, e.g., $-NH_2$ [27]. The increase in the C content results likely from slower decomposition in comparison with other elements [28].

The decrease of *O:C* with the T rise might be also attributed to the loss of hydrophilic surfaces [29]. In addition, the C losses were smaller than in the case of O. The decrease in *H:C* results similarly as the decrease in the content of *O:C* from the faster decomposition of substances containing H in relation to C. The lower values of *O:C* or *H:C* ratios cause the higher energy content of fuel feedstock [30]. Torrefied pruned Oxytree biomass produced at 300 °C and 60 min was characterized by the lowest values of *O:C* and *H:C* of 0.9 and 0.375, respectively. O:C and H:C ratios for wood biomass are >1.4 and >0.65 respectively [30]. For bituminous coal O:C is 1.2 and H:C is 0.125 [31]. The values for the torrefied pruned Oxytree biomass are similar to the value of *Gmelina arborea*, torrefied in the same conditions (300 °C, 60 min) [30].

The standardized regression coefficients β are challenging to interpret because predictors are correlated in each other. For example, when one predictor related to T has a positive impact on the dependent value, the second predictors (e.g., T^2, or T·t), not necessarily. In almost all cases, the correlated predictors had an opposing impact. One common characteristic which can be observed based on β in most of the presented models are that predictors which depended on T had an absolute impact greater than these one related to the time. Based on this, it can be assumed that T has a greater impact on the properties of torrefied pruned biomass of Oxytree.

4.2. Evaluations of the value of torrefied residue biomass

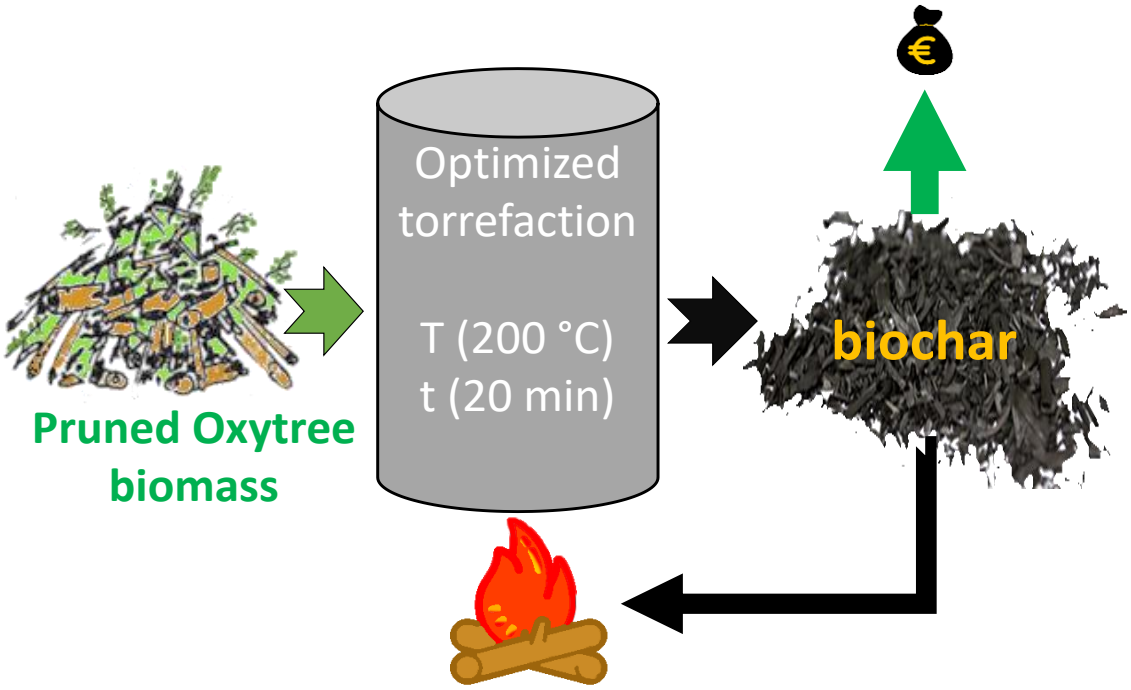

Figure 18. Graphic presentation of the benefits of the pruned Oxytree torrefaction concept.

The common assumption is that the amount of biomass produced during the pruning treatment of the Oxytree plantation is too small to be economically used for energy purposes. Nevertheless, assuming that the material tested in [14] has properties similar to branches (and others residues) that make up waste at Oxytree harvesting (up to 30% of the weight of the tree) a simple model is proposed here for calculating the value of biochar produced in relation to commercial coal fuel available on the market, depending on the T and the duration of the torrefaction process (Figure 18). The model also theoretically calculates the maximum profit from the waste mass on the plantation. The calculations assume that part of the terrified biomass is used to maintain the torrefaction process. Calculations do not include; labor costs, harvesting, transport, processing, and other costs related to the torrefaction process as well as the distribution of produced fuel.

Data for calculations:

- mass of Oxytree residues, Mg; assumed 1 Mg,
- the moisture content of Oxytree residues, %; assumed 50 %,
- torrefaction parameters temperature and time; assumed to be 200 °C and 20 min,

Initial calculations:

Dry mass of Oxytree residues:

$$mr_d = mr_w - mr_w \cdot MC \quad (3)$$

where:

mr_d – dry mass of Oxytree residues, Mg

mr_w – wet mass of Oxytree residues, Mg

MC – moisture content of Oxytree residues, %.

Amount of water in Oxytree residues:

$$m_w = mr_w - mr_d \quad (4)$$

where:

m_w – mass of water in Oxytree residues, Mg.

Main properties of torrefied biomass calculations:

Mass yield of torrefaction based on Figure 3

$$MY = 0.891816 + 0.003525 \cdot T - 0.000013 \cdot T^2 - 0.001684 \cdot t + 0.000062 \cdot t^2 - 0.000025 \cdot T \cdot t \quad (5)$$

where:
MY – mass yield of torrefaction process, %
T – temperature of torrefaction, °C
t – time of torrefaction, min.

Mass of torrefied biomass after torrefaction

$$mtb = mr_d \cdot MY \quad (6)$$

where:
mtb – mass of torrefied biomass after torrefaction process at T, and t conditions.

LHV of torrefied biomass based on figure 10

$$LHV_{tb} = (12394.39 + 0.07 \cdot T^2 + 90.68 \cdot t - 0.79 \cdot t^2)/1000 \quad (7)$$

where:
LHV_{tb} – low heating value of torrefied biomass in dependence of torrefaction conditions, MJ·kg^{-1}
1000 – conversion of kJ to MJ.

Total energy in torrefied biomass

$$E_{tb} = MY \cdot LHV \cdot 1000 \quad (8)$$

where:
E_{tb} – energy in torrefied biomass, kJ
1000 – conversion of Mg to kg.

Energy need to torrefaction process [32]*:*

Data for calculations:

- T_a – ambient temperature, °C, assumed 15 °C,
- T_b – boiling point of water, 100 °C,
- latent heat of water vaporization, 2500 kJ·kg^{-1} [33],
- specific heat of water, 4.18 kJ·kg^{-1} [33],
- specific heat of wood, kJ·kg^{-1}, assumed 1.6 kJ·kg^{-1} [34].

Energy needed to heat a water contained in Oxytree residues

$$E_w = m_w \cdot Cp_{water} \cdot (T_b - T_a) \quad (9)$$

where:
Ew – energy needed to heat water contained in Oxytree residues, MJ
Cp_{water} – specific heat of water, 4.18 kJ·kg^{-1}.

Energy needed to water vaporization

$$E_{ev} = m_w \cdot L_h \quad (10)$$

where:
Eev – energy needed to vaporization of water contained in Oxytree residues, MJ
L_h – latent heat of water vaporization, kJ·kg^{-1}.

Energy needed to heat Oxytree residues during torrefaction

$$E_{hw} = mr_d \cdot Cp_{wood} \cdot (T - T_a) \quad (11)$$

where:
Ehw – energy needed to heat Oxytree residues from ambient to torrefaction temperature, MJ
Cp_{wood} – specific heat of wood, kJ·kg^{-1}.

Total energy needed to torrefied Oxytree residues

$$E = E_w + E_{ev} + E_{hw} \quad (12)$$

where:

E – energy needed to torrefied Oxytree residues

Estimation of the value of torrefied biomass

Estimation was done based on the price of commercial coal fuel available in Poland's market in 2019 and its *LHV*. The value in PLN has been converted to € at the current exchange rate.

Data for calculations:

- Price of commercial coal fuel, €·Mg^{-1}, assumed 170 €·Mg^{-1} [35],
- *LHV* of commercial coal fuel, MJ·kg^{-1}, assumed 23 MJ·kg^{-1} [35],

The estimated value of torrefied biomass

$$V_{tb} = \frac{V_{ccf} \cdot LHV_{tb}}{LHV_{ccf}} \quad (13)$$

where:

V_{tb} – estimated value of torrefied biomass, €·Mg^{-1}

Vccf – value (price) of commercial coal fuel, €·Mg^{-1}

LHV_{ccf} – low heating value of commercial coal fuel, MJ·kg^{-1}.

Profit from torrefied Oxytree residues

Mass of torrefied Oxytree residues net (when assumed that part of it is used as fuel to the process of torrefaction)

$$mtb_n = \frac{E_{tb} - E}{LHV_{tb}} \quad (14)$$

where:

mtb_n – mass of torrefied Oxytree residues net, Mg.

The evaluations of the value of torrefied biomass has been done for 1 Mg of Oxytree wet residues. The moisture content in Oxytree residues was assumed as 50 %. Based on Solver a Microsoft Excel add-in program, the best conditions to torrefaction process were T = 200 °C, and t = 20 min. For this conditions, *MY* of torrefied biomass was 97 %, and *LHV* of torrefied biomass was 16.7 MJ·kg^{-1}. In these conditions calculated value of produced torrefied biomass was 123.38 €·Mg^{-1} d.m., while the net mass obtained after torrefaction was 0.39 Mg d.m. Evaluated value of torrefied biomass from 1 Mg of Oxytree wet residues (containing 50 % of moisture) was 44.92 €.

The presented simple model of evaluation of the value of torrefied Oxytree residues as a fuel is the first step to the evaluation of the profitability of utilization of torrefaction technology to Oxytree residues. The model has been based on simple assumptions, and thus it cannot be used as a fully-fledged tool to evaluate of economical value of torrefied biomass yet. For prices of fuel such as coal, the impact has many factors, such as ash content, grindability, fraction, etc. Nevertheless, after knowing these factors and their impact on the price of coal, the presented model could be extended and improved. The same situation is with the estimations of the cost of production of torrefied biomass. Improved and a more complete analysis of all types of costs is warranted.

5. Conclusions

Presented models of mass yield, energy yield, energy densification ratio, *HHV*, and *LHV* are characterized by $R^2 > 0.78$. Thus, the newly developed models could be used for describing the process of torrefaction of biomass originating from Oxytree pruning. The other models, still describe the process trends well, albeit with large standard deviations in the measurement data. The energetic properties of torrefied Oxytree biomass are comparable to other woody biomass. The highest *HHV* of torrefied biomass was 21 MJ·kg^{-1}, at 300 °C and 20 min. The study found that the most beneficial

Peer-reviewed version available at Materials 2019, 12, ; doi:10.3390/ma12142228

economic aspect parameters of torrefaction are 200 °C and 20 min. These parameters provide the greatest profit and the smallest energetic losses.

Supplementary Materials: The following are available online at https://doi.org/10.3390/data4020055, file: data-04-00055-s001.xlsx. This file contains data of fuel properties of torrefied pruned biomass of Paulownia Clon in Vitro 112 (Oxytree) the hybrid of Paulownia elongata x Paulownia fortunei. The "Read me" sheet is a guide on how to read the data with short information about each type of treatment. The second spreadsheet ("Oxytree biomass yield") contains data about the oxytree biomass yield, energy densification ratio, mass and energy yield of biochars. The third spreadsheet ("Oxytree torrefaction TGA") contains raw data from TGA tests. The fourth spreadsheet ("Proximate analyses") contains information about moisture content, organic matter content, combustible content, and ash content in raw and torrefied oxytree biomass. The fifth spreadsheet ("Ultimate analyses") presents the elemental composition and H:C, and O:C ratio of raw oxytree biomass and biochars, high heating value, low heating value, and high heating value (without ash).

Author Contributions: conceptualization, K.S. and A.B.; methodology, K.S. and A.B.; software, K.S.; validation, K.S., A.B. and J.K.; formal analysis, K.S.; investigation, K.S. M.L., P.B.; resources, K.S., M.L., P.B., A.B., and J.K.; data curation, K.S.; writing—original draft preparation, K.S.; writing—review and editing, K.S., A.B, J.K.; visualization, K.S.; supervision, A.B., and J.K.; project administration, A.B.; funding acquisition, K.S., A.B., and J.K.

Funding: Authors would like to thank „The PROM Programme - International scholarship exchange of PhD candidates and academic staff" is cofinanced by the European Social Fund under the Knowledge Education Development Operational Programme PPI/PRO/2018/1/00004/U/001. Authors would like also to thank the Fulbright Foundation for funding the project titled "Research on pollutants emission from Carbonized Refuse Derived Fuel into the environment," completed at the Iowa State University. In addition, this project was partially supported by the Iowa Agriculture and Home Economics Experiment Station, Ames, Iowa. Project no. IOW05556 (Future Challenges in Animal Production Systems: Seeking Solutions through Focused Facilitation) sponsored by Hatch Act and State of Iowa funds.

Conflicts of Interest: "The authors declare no conflict of interest."

Appendix A

Table A1. Statistic evaluation of 3D model parameters of *HHV* (model 1)

$HHV = a_1+a_2 \cdot T+a_3 \cdot T^2+a_4 \cdot t+a_5 \cdot t^2+a_6 \cdot T \cdot t$, $R^2 = 0.79$, AIC = 8128 red font signifies statistical significance ($p < 0.05$)						
Intercept/coefficient	Value of intercept/ coefficient	Standard error	p	Lower limit of confidence	Upper limit of confidence	Standardized β coefficient
a_1	15766.51	1816.820	8.67808	0.000000	12195.46	-
a_2	-6.93	14.197	-0.48833	0.625567	-34.84	-0.19
a_3	0.07	0.028	2.46019	0.014282	0.01	0.94
a_4	60.04	17.365	3.45749	0.000600	25.91	0.78
a_5	-0.67	0.148	-4.50308	0.000009	-0.96	-0.70
a_6	0.07	0.050	1.33485	0.182637	-0.03	0.23

Table A2. Statistic evaluation of 3D model parameters of *LHV* (model 1)

$LHV = a_1+a_2 \cdot T+a_3 \cdot T^2+a_4 \cdot t+a_5 \cdot t^2+a_6 \cdot T \cdot t$, $R^2 = 0.82$, AIC = 8137 red font signifies statistical significance ($p < 0.05$)						
Intercept/coefficient	Value of intercept/ coefficient	Standard error	p	Lower limit of confidence	Upper limit of confidence	Standardized β coefficient
a_1	14913.84	1835.747	0.000000	11305.59	18522.09	-
a_2	-16.21	14.345	0.259123	-44.41	11.99	-0.40
a_3	0.09	0.028	0.001152	0.04	0.15	1.14
a_4	64.87	17.546	0.000247	30.38	99.35	0.76

a_5	-0.79	0.150	0.000000	-1.09	-0.50	-0.75
a_6	0.10	0.051	0.042425	0.00	0.20	0.32

Table A3. Statistic evaluation of 3D model parameters of *LHV* (model 2)

$LHV = a_1+a_2 \cdot T^2+a_3 \cdot t+a_4 \cdot t^2+a_5 \cdot T \cdot t$, $R^2 = 0.82$, AIC = 8135 red font signifies statistical significance ($p < 0.05$)						
Intercept/coefficient	Value of intercept/ coefficient	Standard error	p	Lower limit of confidence	Upper limit of confidence	Standardized β coefficient
a_1	12877.28	348.9176	0.000000	12191.48	13563.09	-
a_2	0.06	0.0043	0.000000	0.05	0.07	0.75
a_3	66.89	17.4595	0.000147	32.58	101.21	0.78
a_4	-0.79	0.1501	0.000000	-1.09	-0.50	-0.75
a_5	0.10	0.0502	0.058891	0.00	0.19	0.30

Table A4. Statistic evaluation of 3D model parameters of H:C (model 1)

$H:C = a_1+a_2 \cdot T+a_3 \cdot T^2+a_4 \cdot t+a_5 \cdot t^2+a_6 \cdot T \cdot t$, R2 = 0.82, AIC = 164 red font signifies statistical significance ($p < 0.05$)						
Intercept/coefficient	Value of intercept/ coefficient	Standard error	p	Lower limit of confidence	Upper limit of confidence	Standardized β coefficient
a_1	3.576069	0.780513	0.000010	2.032757	5.119380	-
a_2	-0.007620	0.006099	0.213674	-0.019680	0.004440	-0.84
a_3	0.000004	0.000012	0.731624	-0.000020	0.000028	0.23
a_4	-0.011341	0.007460	0.130728	-0.026092	0.003409	-0.60
a_5	0.000200	0.000064	0.002132	0.000074	0.000326	0.85
a_6	-0.000044	0.000022	0.041243	-0.000087	-0.000002	-0.62

References

1. Baležentis, T.; Streimikiene, D.; Zhang, T.; Liobikiene, G. The role of bioenergy in greenhouse gas emission reduction in EU countries: An Environmental Kuznets Curve modelling. *Resour. Conserv. Recycl.* **2019**, *142*, 225–231. doi.org/10.1016/j.resconrec.2018.12.019.
2. Paredes-Sánchez, J.P.; López-Ochoa, L.M.; López-González, L.M.; Las-Heras-Casas, J.; Xiberta-Bernat, J. Evolution and perspectives of the bioenergy applications in Spain. *J. Clean. Prod.* **2019**, *213*, 553–568. doi.org/10.1016/j.jclepro.2018.12.112.
3. Söderberg, C.; Eckerberg, K. Forest Policy and Economics Rising policy conflicts in Europe over bioenergy and forestry. *For. Policy Econ.* **2013**, *33*, 112–119. doi.org/10.1016/j.forpol.2012.09.015.
4. Di Fulvio, F.; Forsell, N.; Korosuo, A.; Obersteiner, M.; Hellweg, S. Spatially explicit LCA analysis of biodiversity losses due to different bioenergy policies in the European Union. *Sci. Total Environ.* **2019**, *651*, 1505–1516. doi.org/10.1016/j.scitotenv.2018.08.419.
5. Liszewski, M.; Bąbelewski, P. Oxytree plantation – second year of research. *Biomasa* **2018**, *8*, 36 – 38.
6. Jakubowski, M.; Tomczak, A.; Jelonek, T. The use of wood and the possibility of planting trees of the paulownia genus. *Acta Sci. Pol. Silv. Colendar. Ratio Ind. Lignar.* **2018**, *17*, 291–297. doi.org/10.17306/J.AFW.2018.4.2018.4.26
7. Paulownia Bulletin ≠ 3 Advices And Instructions Paulownia For Biomass Production Available online: http://paulowniatrees.eu/products/paulownia-planting-material/ (accessed on Mar 12, 2019).
8. Hugo Durán Zuazo, V.; Antonio Jiménez Bocanegra, J.; Perea Torres, F.; Rodríguez Pleguezuelo, C.R.;

Francia Martínez, J.R. Biomass Yield Potential of Paulownia Trees in a Semi-Arid Mediterranean Environment (S Spain). *Int. J. Renew. Energy Res.* **2013**, *3*.

9 Jabłoński, D. Oxytree: Wood for processing in a sawmill 6 years after planting Available online: https://www.drewno.pl/artykuly/10535,oxytree-drewno-do-przerobu-w-tartaku-w-6-lat-od-posadzenia-drzewa.html (accessed on Mar 12, 2019).

10. Dyjakon, A. The Influence of Apple Orchard Management on Energy Performance and Pruned Biomass Harvesting for Energetic Applications. *Energies* **2019**, *12*, 632. doi.org/10.3390/en12040632.

11. Basu, P. *Biomass Gasification, Pyrolysis and Torrefaction*, 2nd ed,; Academic Press, 2013; 87–145, ISBN 978-0-12-396488-5.

12. Chen, W.H.; Peng, J.; Bi, X,T. A state-of-the-art review of biomass torrfeaction, densification and applications. *Renew Susr Energ Rev* **2015**, *44*, 847–866. doi.org/10.1016/j.rser.2014.12.039.

13. Jakubiak, M.; Kordylewski, W. Biomass torrefaction. *Arch. spalania* **2010**, *10*, 11–25.

14. Świechowski, K.; Liszewski, M.; Bąbelewski, P.; Koziel, J.A.; Białowiec A. Fuel Properties of Torrefied Biomass from Pruning of Oxytree. *Data* **2019**, *4*, 1–9. doi:10.3390/data40200556.

15. Stegenta, S.; Kałdun, B.; Białowiec, A. Model selection and determination of kinetic parameters of respiratory activity of wastes during the aerobic process of biostabilization of municipal solid waste fraction. *Rocz. Ochr. Środowiska* **2016**, *18*, 800–814.

16. Wang, L.; Barta-Rajnai, E.; Skreiberg, O.; Khalil, R.; Czégény, Z.; Jakab, E.; Barta, Z.; Grønli, M. Impact of Torrefaction on Woody Biomass Properties. *Energy Procedia* **2017**, *105*, 1149–1154. 10.1016/j.egypro.2017.03.486.

17. Szymon, S.; Adrian, Ł.; Piersa, P.; Romanowska-Duda, Z.; Grzesik, M.; Cebula, A.; Kowalczyk, S. Renewable Energy Sources: Engineering, Technology, Innovation. *Springer International Publishing AG* **2018**, 365–373. doi.org/10.1007/978-3-319-72371-6_35.

18. Tumuluru, J.S.; Sokhansanj, S.; Hess, J.R.; Wright, C.T.; Boardman, R.D. A review on biomass torrefaction process and product properties for energy applications. *Ind. Bioterchnol.* **2011**, *7*, 384-373. doi: 10.1089/ind.2011.7.384.

19. Wang, L.; Barta-Rajnai, E.; Skreiberg; Khalil, R.; Czégény, Z.; Jakab, E.; Barta, Z.; Grønli, M. Effect of torrefaction on physiochemical characteristics and grindability of stem wood, stump and bark. *Appl. Energy* **2018**, *227*, 137–148. doi.org/10.1016/j.apenergy.2017.07.024.

20. Pach, M.; Zanzi, R.; Bjornbom, E. Torrefied biomass a substitute for wood and charcoal . *6th Asia-Pacific Int. Symp. Combust. Energy Util.* **2002**.

21. Khazraie Shoulaifar, T.; Demartini, N.; Zevenhoven, M.; Verhoeff, F.; Kiel, J.; Hupa, M. Ash-forming matter in torrefied birch wood: Changes in chemical association. *Energy and Fuels* **2013**, *27*, 5684–5690. doi.org/10.1021/ef4005175.

22. Tumuluru, J.S. Comparison of Chemical Composition and Energy Property of Torrefied Switchgrass and Corn Stover. *Front. Energy Res.* **2015**, *3*, 1–11. doi: 10.3389/fenrg.2015.00046.

23. Grams, J.; Kwapińska, M.; Jędrzejczyk, M.; Rzeźnicka, I.; Leahy, J.J.; Ruppert, A.M. Surface characterization of Miscanthus × giganteus and Willow subjected to torrefaction. *J. Anal. Appl. Pyrolysis* **2019**, *138*, 231–241. doi.org/10.1016/j.jaap.2018.12.028.

24. Rodrigues, A.; Loureiro, L.; Nunes, L.J.R. Torrefaction of woody biomasses from poplar SRC and Portuguese roundwood: Properties of torrefied products. *Biomass and Bioenergy* **2018**, *108*, 55–65. doi.org/10.1016/j.biombioe.2017.11.005.

25. Li, S.; Harris, S.; Anandhi, A.; Chen, G. Predicting biochar properties and functions based on feedstock

and pyrolysis temperature: A review and data syntheses. *J. Clean. Prod.* **2019**, *215*, 890–902. doi.org/10.1016/j.jclepro.2019.01.106.

26. Lu, J.J.; Chen, W.H. Product yields and characteristics of corncob waste under various torrefaction atmospheres. *Energies* **2014**, *7*, 13–27. doi: 10.3390/en7010013.
27. Li, S.; Chen, G. Thermogravimetric, thermochemical, and infrared spectral characterization of feedstocks and biochar derived at different pyrolysis temperatures. *Waste Manag.* **2018**, *78*, 198–207. doi.org/10.1016/j.wasman.2018.05.048.
28. Li, S.; Barreto, V.; Li, R.; Chen, G.; Hsieh, Y.P. Nitrogen retention of biochar derived from different feedstocks at variable pyrolysis temperatures. *J. Anal. Appl. Pyrolysis* **2018**, *133*, 136–146 doi.org/10.1016/j.jaap.2018.04.010.
29. Novak, J.; Lima, I.; Xing, B.; Gaskin, J.W.; Steiner, C.; Das, K.C.; Ahmedna, M.; Rehrah, D.; Watts, D.W.; Busscher, W.J.; et al. Characterization of designer biochar produced at different temperatures and their effects on a loamy sand. *Ann. Environ. Sci.* **2009**, *3*, 195–206.
30. Akanni, A.A.; Kolawole, O.J.; Dayanand, P.; Ajani, L.O.; Madhurai, M. Influence of torrefaction on lignocellulosic woody biomass of Nigerian origin. *J. Chem. Technol. Metall.* **2019**, *54*, 274–285.
31. Markič, M.; Kalan, Z.; Pezdič, J.; Faganeli, J. H/C versus O/C atomic ratio characterization of selected coals in Slovenia. *Geologija* **2011**, *50*, 403–426 doi:10.5474/geologija.2007.028.
32. Bialowiec, A.; Boer, E. Den; Boer, J. Den; Cenian, A. *Innovations in waste management. Selected issues*; 2018; ISBN 9788377172780. doi: 10.30825/1.3.2018.
33. Brusseau, M.L.; Walker, D.B.; Fitzsimmons, K. *Physical-Chemical Characteristics of Water*; 3rd ed.; Elsevier Inc., 2019; ISBN 9780128147191. doi.org/10.1016/B978-0-12-814719-1.00003-3.
34. Radmanović, K.; Đukić, I.; Pervan, S. Specific Heat Capacity of Wood. *Drv. Ind.* **2014**, *65*, 151–157. doi:10.5552/drind.2014.1333.
35. Available online: https://www.wnp.pl/gornictwo/notowania/ceny_wegla_pgg/ (accessed on Mar 12, 2019).